On the adaptive Levin method

Shukui Chen[1*], Kirill Serkh[1,2*] and James Bremer[2*]

[1*]Department of Computer Science, University of Toronto.

[2]Department of Mathematics, University of Toronto.

*Corresponding author(s). E-mail(s): bremer@math.toronto.edu;

Abstract

The Levin method is a well-known technique for evaluating oscillatory integrals, which operates by solving a certain ordinary differential equation in order to construct an antiderivative of the integrand. It was long believed that this approach suffers from "low-frequency breakdown," meaning that the accuracy of the calculated value of the integral deteriorates when the integrand is only slowly oscillating. Recently presented experimental evidence, however, suggests that if a Chebyshev spectral method is used to discretize the differential equation and the resulting linear system is solved via a truncated singular value decomposition, then no low-frequency breakdown occurs. Here, we provide a proof that this is the case, and our proof applies not only when the integrand is slowly oscillating, but even in the case of stationary points. Our result puts adaptive schemes based on the Levin method on a firm theoretical foundation and accounts for their behavior in the presence of stationary points. We go on to point out that by combining an adaptive Levin scheme with phase function methods for ordinary differential equations, a large class of oscillatory integrals involving special functions, including products of such functions and the compositions of such functions with slowly-varying functions, can be easily evaluated without the need for symbolic computations. Finally, we present the results of numerical experiments which illustrate the consequences of our analysis and demonstrate the properties of the adaptive Levin method.

1 Introduction

The Levin method, which was introduced in [1], is a classical technique for evaluating integrals of the form

$$\int_a^b f(x)\exp(ig(x))\,dx, \tag{1}$$

where f is slowly varying, g is real-valued and slowly varying and g' is of large magnitude. It operates by solving the ordinary differential equation

$$p'(x) + ig'(x)p(x) = f(x) \tag{2}$$

in order to find a function p such that

$$\frac{d}{dx}\left(p(x)\exp(ig(x))\right) = f(x)\exp(ig(x)). \tag{3}$$

The value of the integral (1) is then equal to

$$p(b)\exp(ig(b)) - p(a)\exp(ig(a)). \tag{4}$$

Under the assumptions made above, (2) admits a slowly-varying solution p_0, which means that (1) can be computed rapidly. Moreover, although the differential operator

$$L\left[p\right](x) = p'(x) + ig'(x)p(x) \tag{5}$$

appearing on the left-hand side of (2) has a one-dimensional nullspace consisting of all multiples of the function $\eta(x) = \exp(-ig(x))$, the equation (2) can still be solved accurately via a spectral collocation method if some care is taken. In particular, as long as the chosen grid of collocation nodes is dense enough to resolve f and g', but not sufficiently dense to resolve η, the matrix discretizing the differential operator L will be well-conditioned and inverting it will result in a high-accuracy approximation of the slowly-varying solution p_0.

When the magnitude of g' is sufficiently small, any grid of collocation nodes dense enough to resolve f and g' will also resolve η. As a consequence, the corresponding spectral discretization of L will have a small singular value and numerical difficulties can arise in the course of solving (2). This phenomenon is known as "low-frequency breakdown," and it was commonly considered to be a significant limitation of Levin methods. The recent articles [2, 3] present experimental evidence showing that, when Chebyshev spectral methods are used to discretize the differential equation (2) and the resulting linear system is solved via a truncated singular value decomposition, no low-frequency breakdown seems to occur.

Here, we prove that this is the case. We first show that, when g' is nonvanishing, the Levin equation admits a well-behaved solution that can be approximated by a polynomial expansion at a cost which depends on a measure of the complexity of f, g' and the inverse function g^{-1} of g, as well as the ratio of the maximum and minimum absolute values of g', but not on the magnitude of

g'. This result improves on those presented in [1] and its follow-up [4] by handling the case in which g' is of positive, but arbitrarily small, magnitude and by explicitly showing that the cost of representing the well-behaved solution of the Levin equation via a polynomial expansion is independent of the magnitude of g' (note that the assumptions made in both [1] and [4] fail to hold when g' is of sufficiently small positive magnitude). We then consider the case in which g' is of small magnitude, possibly with zeros. In this event, g need not be invertible, but we show that the Levin equation nonetheless admits a well-behaved solution, and that this solution can be approximated by a polynomial expansion at a cost which decreases as the magnitude of g' decreases. We use these two results to prove that, when the Levin equation is discretized via a Chebyshev spectral collocation method and the resulting linear system is solved using a truncated singular value decomposition, high accuracy is obtained regardless of the magnitude of g' and whether or not g' has zeros. We note that our analysis also improves on the analysis of [5], in which the authors prove that there exists a solution p to the Levin equation such that $\|p'\|_{L^2([a,b])} = \mathcal{O}(\|g'\|_{L^\infty([a,b])}^{-1/(k+1)})$ on an interval containing a stationary point of order k, for which they provide initial conditions, since their solution can have higher order derivatives which grow with $\|g'\|_{L^\infty([a,b])}$.

One implication of the absence of low-frequency breakdown is that the Levin method can be used as the basis of an adaptive integration scheme — since adaptive subdivision reduces the effective magnitude of g', such an approach requires that the method remain accurate regardless of the magnitude of g'.

An adaptive Levin scheme of this kind, based on collocation at Chebyshev points, was proposed by Moylan in [6]. It was shown to be effective in the presence of stationary points, before the absence of low-frequency breakdown was directly observed in [2, 3]. Another adaptive Levin scheme was later proposed in [7], which uses collocation points in the vicinity of the endpoints to attain higher asymptotic orders in the magnitude of g', on those intervals where g' is of large magnitude. Unlike Moylan's scheme, the method of [7] assumes that the locations of the stationary points are known in advance.

One distinctive feature of Moylan's scheme is that it is based on a more general version of the Levin method introduced in [8]. In particular, the integrand is of the form

$$\int_a^b \mathbf{w}(x) \cdot \mathbf{f}(x)\, dx \tag{6}$$

with $\mathbf{f}\colon [a,b] \to \mathbb{C}^n$ slowly varying and $\mathbf{w}\colon [a,b] \to \mathbb{C}^n$ a solution of a system of ordinary differential equations

$$\mathbf{w}'(x) = \mathscr{A}(x)\mathbf{w}(x) \tag{7}$$

whose coefficient matrix $\mathscr{A}\colon [a,b] \to \mathbb{C}^{n\times n}$ is also slowly varying. The scheme of [8] operates by finding a slowly-varying vector field $\mathbf{F}\colon [a,b] \to \mathbb{C}^n$ satisfying

the system of differential equations

$$\mathbf{F}'(x) + \mathscr{A}(x)^t \mathbf{F}(x) = \mathbf{f}(x) \tag{8}$$

and evaluating (6) via the formula

$$\mathbf{F}(b) \cdot \mathbf{w}(b) - \mathbf{F}(a) \cdot \mathbf{w}(a). \tag{9}$$

Moylan's algorithm adaptively decomposes the domain of an oscillatory integral and uses the above formulation of the Levin method to evaluate it over each subinterval. An implementation of this scheme using Wolfram's Mathematica package is described in [6], and experimental evidence showing that it works well in practice in the low-frequency regime, and even in the case of stationary points, is presented. However, all of the estimates discussed in [6] break down in the low-frequency regime. Moreover, the implementation of the adaptive Levin method described in [6] relies heavily on symbolic and arbitrary precision computations, including in the solution of the linear system which arises when (8) is discretized.

One advantage of the Moylan scheme over an adaptive scheme based on the formulation of [1] is the great generality of the integrands which can be expressed as solutions of systems of the form (7) with slowly-varying coefficient matrices. However, most oscillators of interest are solutions of scalar differential equations of the form

$$y^{(n)}(t) + q_{n-1}(t) y^{(n-1)}(t) + \cdots + q_1(t) y'(t) + q_0(t) y(t) = 0 \tag{10}$$

whose coefficients are slowly varying, and it is well known that such equations admit slowly-varying phase functions. More explicitly, under mild conditions on the coefficients $q_0, \ldots, q_{n-1}$, there exist slowly-varying $\psi_1, \ldots, \psi_n$ such that

$$\{\exp(\psi_j(t)) : j = 1, \ldots, n\} \tag{11}$$

is a basis in the space of solutions of (10). This observation underlies the WKB method and almost all other techniques for the asymptotic approximation of solutions of ordinary differential equations in the high-frequency regime (see, for instance, [9], [10] and [11, 12, 13]). See also [14], which contains a careful proof of the existence of slowly-varying phase functions for second order differential equations that can be extended to the case of higher order scalar equations without too much difficulty. A numerical algorithm for constructing slowly-varying phase functions for scalar equations of the form (10) in time independent of frequency is described in [15]. Specialized methods for the case of second order linear ordinary differential equations are described in [16] and [17]. Because many oscillators of interest satisfy second order linear ordinary differential equations (e.g., Bessel functions, Jacobi polynomials, spheroidal wave functions and Hermite polynomials), the experiments of this article focus on this case and we use the algorithm of [17] in order to construct the necessary slowly-varying phase functions.

The existence of slowly-varying phase functions for scalar differential equations and the ability to rapidly compute them via the numerical schemes of [15, 16, 17] imply that an adaptive method based on Levin's original formulation suffices to evaluate a huge class of oscillatory integrals. Moreover, when phase-function representations of oscillators have been computed, integrals involving the products of oscillators or the composition of an oscillator with a slowly-varying function can be evaluated in a straightforward fashion. This is in contrast to Moylan's adaptive scheme, which requires knowledge of a system of differential equations satisfied by whatever combination of oscillators is being considered. Moylan's scheme relies heavily on Mathematica's symbolic capabilities to derive the necessary differential equations in such situations.

The remainder of this article is structured as follows. Section 2 discusses the requisite mathematical and numerical preliminaries. Section 3 contains our analysis showing that the Levin equation always admits a well-behaved solution. In Section 4, we use the results of Section 3 to establish that no accuracy is lost when a Chebyshev collocation scheme is used to discretize the Levin equation and the resulting system of linear equations is solved via a truncated singular value decomposition. In Section 5, we give a detailed description of the adaptive Levin method. In Section 6, we discuss phase function methods for second order linear ordinary differential equations. In Section 7, we present the results of numerical experiments conducted to demonstrate the properties of the adaptive Levin method. Finally, we close with a few brief remarks in Section 8.

2 Preliminaries

2.1 Notation and conventions

We use capital script letters such as $\mathscr{A}$ for matrices, and the names of vectors are displayed using a bold font. We denote by $L^\infty(\Omega)$ the Banach space of functions which are essentially bounded on the Lebesgue measurable subset Ω of $\mathbb{R}$, and by $C^n([a,b])$ the Banach space of functions $(a,b) \mapsto \mathbb{C}$ whose derivatives through order n are uniformly continuous and hence admit continuous extensions to $[a,b]$. We denote by $M([a,b])$ the Banach space of complex Radon measures on $[a,b]$, which is the dual of $C^0([a,b])$, and by $|\mu|$ the total variation of $\mu \in M([a,b])$. The notation $\|x\|_X$ is used for the norm of an element x of one of the Banach spaces X mentioned above. The Euclidean norm of a vector $\mathbf{x} \in \mathbb{C}^n$ is $\|\mathbf{x}\|_2$, and $\|\mathscr{A}\|_2$ is the $\mathbb{C}^n \to \mathbb{C}^n$ Euclidean operator norm of the $n \times n$ matrix $\mathscr{A}$.

We denote by $C^\infty([a,b])$ the set of functions which are infinitely differentiable and whose derivatives of all orders are uniformly continuous on (a,b), and use $S(\mathbb{R})$ for the Schwartz space of infinitely differentiable functions whose derivatives of all orders are rapidly decaying functions. The space of tempered distributions is $S'(\mathbb{R})$. We often write $\langle \varphi, f \rangle$ for the action of the tempered distribution φ on the function $f \in S(\mathbb{R})$, although we occasionally use other

notations for this when their meanings are clear. The support of $\varphi \in S'(\mathbb{R})$ is the complement of the union of all open sets U such that $\langle \varphi, f \rangle = 0$ whenever $f \in S(\mathbb{R})$ has support contained in U. The order of a tempered distribution φ is the least nonnegative integer n with the property that for each compact set $K \subset \mathbb{R}$ there exists a constant M_K such that

$$|\langle \varphi, f \rangle| \leq M_K \sup_{0 \leq k \leq n} \sup_{x \in K} \left| D^k f(x) \right| \tag{12}$$

for every function $f \in S(\mathbb{R})$ whose support is contained in K (we note that every tempered distribution has finite order). The space of tempered distributions of order n which are supported on $[a, b]$ can, of course, be identified with the dual space of $C^n([a, b])$.

We use the convention

$$\widehat{f}(\xi) = \frac{1}{2\pi} \int_{-\infty}^{\infty} f(x) \exp(-i\xi x)\, dx \tag{13}$$

for the Fourier transform of $f \in S(\mathbb{R})$ (this is slightly nonstandard, but quite convenient when discussing the Levin equation). Of course, $\widehat{f} \in S(\mathbb{R})$ and we have

$$f(x) = \int_{-\infty}^{\infty} \widehat{f}(\xi) \exp(i\xi x)\, d\xi. \tag{14}$$

We extend the Fourier transform to a mapping $S'(\mathbb{R}) \to S'(\mathbb{R})$ in the usual way, via the formula $\langle \widehat{\varphi}, g \rangle = \langle \varphi, \widehat{g} \rangle$. If φ is compactly supported on $[a, b]$, then its Fourier transform coincides with the function $\widehat{\varphi}(\xi) = \langle \varphi, \eta_\xi \rangle$, where $\eta_\xi(x) = 1/(2\pi) \exp(-i\xi x)$. The Schwartz-Paley-Wiener theorem asserts that $\widehat{\varphi}$ is entire in this case, and gives bounds on its growth at infinity. Likewise, if $\widehat{\varphi}$ is compactly supported on $[a, b]$, then φ is the entire function defined via the formula $\varphi(x) = \langle \widehat{\varphi}, \nu_x \rangle$ with $\nu_x(\xi) = \exp(i\xi x)$. If the Fourier transform of φ is supported on the finite interval $[-c, c]$, then we say that φ has bandlimit c. Note that we do not require that c be the smallest positive real number with this property.

The notation $x \lesssim y$ indicates that there is some constant $C > 0$ not depending on either x or y, such that $x \leq Cy$.

2.2 Chebyshev interpolation

We use T_n to denote the Chebyshev polynomial of degree n and

$$-1 = x_{1,k}^{\text{cheb}} < x_{2,k}^{\text{cheb}} < \ldots < x_{k,k}^{\text{cheb}} = 1 \tag{15}$$

for the k-point grid of extremal Chebyshev nodes on the interval $[-1, 1]$. That is,

$$x_{j,k}^{\text{cheb}} = \cos\left(\pi \frac{k-j}{k-1}\right), \quad j = 1, \ldots, k. \tag{16}$$

It is well known that

$$\frac{2}{k-1}\sum_{j=1}^{k}{}''T_n\left(x_{j,k}^{\text{cheb}}\right)T_m\left(x_{j,k}^{\text{cheb}}\right)=\begin{cases}1, & \text{if } n=m=1,\ldots,k-2,\\ 2, & \text{if } n=m=0,k-1,\\ 0, & \text{if } n\neq m;\ n,m<k,\end{cases} \tag{17}$$

where the double prime symbol after the summation indicates that the first and last term of the series are weighted by 1/2 (this formula can be found, for instance, in Chapter 4 of [18]). If $f\in C^{\infty}([-1,1])$, then we use $\mathsf{P}_k[f]$ to denote the Chebyshev expansion of the form

$$\sum_{n=0}^{k-1}a_nT_n(x) \tag{18}$$

which agrees with f at the nodes (15). It follows from (17) that the coefficients in (18) are given by

$$a_n=\begin{cases}\dfrac{1}{k-1}\displaystyle\sum_{j=1}^{k}{}''T_n\left(x_{j,k}^{\text{cheb}}\right)f\left(x_{j,k}^{\text{cheb}}\right) & \text{if } n=0 \text{ or } n=k-1\\ \dfrac{2}{k-1}\displaystyle\sum_{j=1}^{k}{}''T_n\left(x_{j,k}^{\text{cheb}}\right)f\left(x_{j,k}^{\text{cheb}}\right) & \text{if } n=1,\ldots,k-2.\end{cases} \tag{19}$$

We use the notation $\mathscr{D}_k$ to denote the $k\times k$ spectral differentiation matrix which maps the vector

$$\begin{pmatrix}g\left(x_{1,k}^{\text{cheb}}\right)\\ g\left(x_{2,k}^{\text{cheb}}\right)\\ \vdots\\ g\left(x_{k,k}^{\text{cheb}}\right)\end{pmatrix} \tag{20}$$

of values of an expansion of the form

$$g(x)=\sum_{n=0}^{k-1}a_nT_n(x) \tag{21}$$

at the nodes of the k-point extremal Chebyshev grid to the vector

$$\begin{pmatrix}g'\left(x_{1,k}^{\text{cheb}}\right)\\ g'\left(x_{2,k}^{\text{cheb}}\right)\\ \vdots\\ g'\left(x_{k,k}^{\text{cheb}}\right)\end{pmatrix} \tag{22}$$

of values of the expansion's derivative at the nodes of the k-point extremal Chebyshev grid. We denote by $\mathscr{I}_{2k,k}$ the $2k\times k$ interpolation matrix which

takes the vector

$$\begin{pmatrix} g\left(x_{1,k}^{\text{cheb}}\right) \\ g\left(x_{2,k}^{\text{cheb}}\right) \\ \vdots \\ g\left(x_{k,k}^{\text{cheb}}\right) \end{pmatrix} \tag{23}$$

of values of an expansion of the form (21) at the nodes of the k-point extremal Chebyshev grid to the vector

$$\begin{pmatrix} g\left(x_{1,2k}^{\text{cheb}}\right) \\ g\left(x_{2,2k}^{\text{cheb}}\right) \\ \vdots \\ g\left(x_{2k,2k}^{\text{cheb}}\right) \end{pmatrix} \tag{24}$$

of values of the expansion at the nodes of the $2k$-point extremal Chebyshev grid.

It is well known that if $f \in C^{\infty}([-1,1])$ is infinitely differentiable, then it admits a uniformly convergent Chebyshev series

$$f(x) = \sum_{n=0}^{\infty} b_n T_n(x) \tag{25}$$

such that

$$|b_n| = \mathcal{O}\left(\frac{1}{n^m}\right) \quad \text{as} \quad n \to \infty \tag{26}$$

for all $m \geq 1$. From (17) it is clear that the coefficients $\{b_n\}$ in (25) are related to the coefficients $\{a_n\}$ in the expansion of $\mathsf{P}_k[f]$ through the formula

$$a_n = b_n + b_{n+2(k-1)} + b_{n+4(k-1)} + \dots \,. \tag{27}$$

Since $|T_n(x)| \leq 1$ and $|T_n'(x)| \leq n^2$ for all $x \in [-1,1]$, it follows from (27) that

$$\|\mathsf{P}_k[f] - f\|_{L^{\infty}([-1,1])} \leq 2 \sum_{n=k}^{\infty} |b_n| \tag{28}$$

and

$$\left\|\mathsf{P}_k[f]' - f'\right\|_{L^{\infty}([-1,1])} \leq 2 \sum_{n=k}^{\infty} n^2 |b_n| \,. \tag{29}$$

Obviously, if f is a polynomial of degree less than k, then

$$\mathsf{P}_k[f](x) = f(x) \tag{30}$$

and

$$\mathsf{P}_k\left[f'\right](x) = f'(x) = \mathsf{P}_k\left[f\right]'(x). \tag{31}$$

2.3 Approximation by bandlimited functions

It will often be necessary for us to approximate a function f given on the interval $[-1,1]$ via a "well-behaved" bandlimited function f_b. For us, well-behaved means that the $L^\infty(\mathbb{R})$ norms of f_b, its Fourier transform and the derivative of its Fourier transform are bounded by small constant multiples of the $L^\infty([-1,1])$ norm of f. Moreover, it is desirable to minimize the bandlimit of f_b subject to these constraints.

Under various regularity assumptions on f, it is possible to prove the existence of an approximate satisfying these requirements. The following theorem, which is a slightly modified version of Theorem 1 in [19], is an example of a result of this type which holds under relatively weak regularity conditions on f.

Theorem 1 *Suppose that $f : [-1,1] \to \mathbb{C}$ admits an infinitely differentiable extension to an open neighborhood of $[-1,1]$. Then for each positive integer m and each real number $c > 1$, there exists a constant $K(m,f)$, depending on m and f but not on c, and a function $f_b \in S(\mathbb{R})$ such that*

1. *$\widehat{f_b}$ is supported on $[-c-2, c+2]$,*
2. *$\|f_b - f\|_{L^\infty([-1,1])} \leq \dfrac{K(m,f)}{c^m}$,*
3. *$\|f_b(x)\|_{L^\infty(\mathbb{R})} \leq 2\|f\|_{L^\infty([-1,1])} + \dfrac{K(m,f)}{c^m}$,*
4. *$\left\|\widehat{f_b}(\xi)\right\|_{L^\infty(\mathbb{R})} \leq 4\|f\|_{L^\infty([-1,1])}$ and*
5. *$\left\|\widehat{f_b}'(\xi)\right\|_{L^\infty(\mathbb{R})} \leq 4\|f\|_{L^\infty([-1,1])}$.*

Proof We let $M = \|f\|_{L^\infty([-1,1])}$ and choose $0 < \delta < 1$ such that f is infinitely differentiable on $[-1-\delta, 1+\delta]$ and bounded in magnitude by $2M$ there. We take T_1 to be an infinitely differentiable window function $\mathbb{R} \to \mathbb{R}$ such that $|T_1(x)| \leq 1$ for all $x \in \mathbb{R}$, $T_1(x) = 1$ for all $x \in [-1,1]$ and $T_1(x) = 0$ for all $|x| \geq 1+\delta$. One can construct this function quite easily using the infinitely differentiable ramp function

$$H(x) = \begin{cases} 0, & x < -1, \\ \frac{1}{2}\left(1 + \operatorname{erf}\left(\frac{x}{\sqrt{1-x^2}}\right)\right), & x \in [-1,1], \\ 1, & x > 1, \end{cases} \tag{32}$$

suggested in [19]. Then $f_1(x) = f(x)T_1(x)$ is an element of the space $S(\mathbb{R})$, and so is its Fourier transform $\widehat{f_1}$. Consequently, there exists a constant k_1 (depending on m and f) such that

$$\left|\widehat{f_1}(\xi)\right| \leq \frac{k_1}{|\xi|^{m+1}}. \tag{33}$$

Since T_1 is bounded in magnitude by 1,

$$|f_1(x)| \leq 2M \quad \text{for all} \quad x \in \mathbb{R}. \tag{34}$$

It follows from this that

$$\left|\widehat{f_1}(\xi)\right| = \left|\frac{1}{2\pi}\int_{-1-\delta}^{1+\delta} f_1(x)\exp(-i\xi x)\,dx\right| \leq \frac{2}{\pi}(1+\delta)M \leq \frac{4}{\pi}M \tag{35}$$

and

$$\left|\widehat{f_1}'(\xi)\right| = \left|\frac{-i}{2\pi}\int_{-1-\delta}^{1+\delta} f_1(x)x\exp(-i\xi x)\,dx\right| \leq \frac{2}{\pi}(1+\delta)^2 M \leq \frac{8}{\pi}M \tag{36}$$

for all $\xi \in \mathbb{R}$.

Now we let T_2 be an infinitely differentiable window function such that $|T_2(x)| \leq 1$ and $\left|T_2'(x)\right| \leq 1$ for all $x \in \mathbb{R}$, $T_2(x) = 1$ for all $x \in [-c, c]$ and $T_2(x) = 0$ for all $|x| > c + 2$. Such a function can be easily constructed using the ramp function H defined in (32). We define f_b by

$$\widehat{f_b}(\xi) = \widehat{f_1}(\xi)T_2(\xi), \tag{37}$$

so that the first of the properties listed above is clearly satisfied. From (33) and the definition of T_2, it is clear that for all $x \in \mathbb{R}$,

$$\begin{aligned} |f_1(x) - f_b(x)| &= \left|\int_{-\infty}^{\infty} \widehat{f_1}(\xi)\,(1 - T_2(\xi))\exp(i\xi x)\,d\xi\right| \\ &\leq \int_{|\xi|>c} \left|\widehat{f_1}(\xi)\right| d\xi \\ &\leq \frac{4k_1}{m\,c^m}. \end{aligned} \tag{38}$$

This inequality establishes the second of the properties of the function f_b listed above and, by combining it with (34), we obtain the third. It follows from (35), (36) and the properties of T_2 that

$$\left|\widehat{f_b}(\xi)\right| = \left|\widehat{f_1}(\xi)T_2(\xi)\right| \leq \frac{4}{\pi}M \tag{39}$$

and

$$\left|\widehat{f_b}'(\xi)\right| = \left|\widehat{f_1}'(\xi)T_2(\xi) + \widehat{f_1}(\xi)T_2'(\xi)\right| \leq \frac{4}{\pi}M + \frac{8}{\pi}M = \frac{12}{\pi}M \tag{40}$$

for all $\xi \in \mathbb{R}$. This establishes the last two of the properties of f_b listed above. □

More precise results of this type can be given under stronger regularity assumptions on f. However, the necessary arguments are rather technical and beyond the scope of this paper. Accordingly, now that we have established the existence of a suitable bandlimited approximate under the weak condition that f admits an infinitely differentiable extension in a neighborhood of $[-1, 1]$, we prefer to simply introduce the following definition.

Definition 1 Suppose that $f : [-1, 1] \to \mathbb{C}$ admits an infinitely differentiable extension to an open interval containing $[-1, 1]$. Then, for each real number $0 < \epsilon < 1$, we denote by $c_f(\epsilon)$ the smallest positive real number c such that there exists a function $f_b \in S(\mathbb{R})$ of bandlimit c with the following properties:

1. $\|f - f_b\|_{L^\infty([-1,1])} \leq \epsilon \|f\|_{L^\infty([-1,1])}$,
2. $\|f_b\|_{L^\infty(\mathbb{R})} \leq 4 \|f\|_{L^\infty([-1,1])}$,
3. $\left\|\widehat{f_b}\right\|_{L^\infty(\mathbb{R})} \leq 4 \|f\|_{L^\infty([-1,1])}$ and
4. $\left\|\widehat{f_b}'\right\|_{L^\infty(\mathbb{R})} \leq 4 \|f\|_{L^\infty([-1,1])}$.

The following is an immediate consequence of Theorem 1.

Corollary 1 *If $f : [-1,1] \to \mathbb{C}$ admits an infinitely differentiable extension to a neighborhood of $[-1,1]$, then for every positive integer m, there exists a constant $C(m,f)$ depending only m and f, such that*

$$c_f(\epsilon) \leq C(m,f) \left(\frac{1}{\epsilon}\right)^{\frac{1}{m}}, \tag{41}$$

for all sufficiently small $\epsilon > 0$.

Under the assumption that $f : [-1,1] \to \mathbb{C}$ admits an extension which is bounded and analytic on a horizontal strip containing the real axis, then there clearly exists a constant $C(f)$ such that

$$c_f(\epsilon) \leq C(f) \log\left(\frac{1}{\epsilon}\right) \tag{42}$$

for all sufficiently small $\epsilon > 0$. We conjecture that this also holds when f admits an extension which is analytic in an open neighborhood of $[-1,1]$, but a proof of this is beyond the scope of the present article.

2.4 Legendre expansions of bandlimited functions

The Schwartz-Paley-Wiener theorem asserts that if φ is a tempered distribution whose Fourier transform $\widehat{\varphi}$ has compact support, then φ is, in fact, an entire function satisfying certain growth conditions at ∞. It follows from this and standard results in approximation theory (which can be found in [20], for example) that the Legendre expansion of φ decays superexponentially. Here, for the sake of concreteness, we give a simple bound on the coefficients in the Legendre expansion of φ which depends on the order n of $\widehat{\varphi}$ and its bandlimit c. Throughout this subsection, we use P_k to denote the Legendre polynomial of degree k and j_ν to denote the spherical Bessel function of order ν. Definitions of these functions can be found, for instance, in [21].

Lemma 1 *If φ is a tempered distribution of order n which is supported on $[a,b]$, then there exist complex numbers $c_0, \ldots, c_{n-1}$ and a complex Radon measure μ on*

$[a, b]$ *such that*

$$\langle \varphi, f \rangle = \sum_{k=0}^{n-1} c_k f^{(k)}(a) + \int_a^b f(x)\, d\mu(x), \tag{43}$$

for all $f \in C^n([a, b])$.

Proof Because the space of tempered distributions of order n which are supported on $[a, b]$ can be identified with the dual space of $C^n([a, b])$, it suffices to show that any element of the dual of $C^n([a, b])$ is of the form (43). The case $n = 0$ follows by a trivial application of the Riesz representation theorem, so we suppose that $n \geq 1$. Because any function $f \in C^n([a, b])$ can be written as

$$f(x) = \sum_{k=0}^{n-1} \frac{f^{(k)}(a)}{k!}(x - a)^k + \int_a^x \frac{f^{(n)}(u)}{(n-1)!}(u - a)^{n-1}\, du, \tag{44}$$

the map

$$f \mapsto \left(f(a), f'(a), \ldots, f^{(n-1)}(a), f^{(n)} \right) \tag{45}$$

is an isomorphism from $C^n([a, b])$ to $\mathbb{C}^n \times C([a, b])$. The result now follows from this and the observations that the dual of $C([a, b])$ is the space of complex Radon measures $M([a, b])$ and $\mathbb{C}^n$ is its own dual space. □

Lemma 2 *If the Fourier transform of the tempered distribution* φ *is of order* n *and has support on the interval* $[a, b]$*, then* φ *coincides with an entire function of the form*

$$\varphi(x) = p_{n-1}(x) + x^n \int_a^b e^{i\xi x}\, d\mu(\xi), \tag{46}$$

where p_{n-1} *is a polynomial of degree at most* $n - 1$ *and* $\mu \in M([a, b])$.

Proof The tempered distribution φ is given by

$$\varphi(x) = \langle \widehat{\varphi}, \nu_x \rangle, \tag{47}$$

where $\nu_x(\xi) = \exp(i\xi x)$. The result follows from this and Lemma 1. □

Lemma 3 *For all real-valued* ξ *and nonnegative integers* k*,*

$$\left| \int_{-1}^{1} \exp(i\xi x) P_k(x)\, dx \right| \leq \frac{2 \left| \frac{\xi}{2} \right|^k}{\Gamma(k + 1)}. \tag{48}$$

Proof The formula

$$\int_{-1}^{1} \exp(i\xi x) P_k(x)\, dx = 2i^k j_k(\xi), \tag{49}$$

can be found in Section 7.8 of [22], among many other sources. Combining it with the well-known inequality

$$|j_k(z)| \leq \frac{\left|\frac{z}{2}\right|^k}{\Gamma(k+1)}, \tag{50}$$

which is a special case of Formula 10.14.4 in [21], yields the conclusion of the lemma. □

Theorem 2 *Suppose that the Fourier transform of $\varphi \in S'(\mathbb{R})$ is a tempered distribution of order n supported on the interval $[-c,c]$ with $c \geq 1$. Then φ is an entire function and the coefficients in the Legendre expansion*

$$\varphi(x) = \sum_{m=0}^{\infty} a_m P_m(x) \tag{51}$$

of φ satisfy

$$|a_m| \lesssim \frac{\left(\frac{c}{2}\right)^{m+n}}{\Gamma(m-n+1)}, \tag{52}$$

for all $m \geq n$.

Proof By Lemma 2,

$$\begin{aligned}\int_{-1}^{1} \varphi(x) P_m(x)\,dx = &\int_{-1}^{1} p_{n-1}(x) P_m(x)\,dx \\ &+ \int_{-c}^{c} \left(\int_{-1}^{1} x^n \exp(i\xi x) P_m(x)\,dx \right) d\mu(\xi),\end{aligned} \tag{53}$$

where p_{n-1} is a polynomial of degree at most $n-1$ and $\mu \in M([-c,c])$. For $m \geq n$,

$$\int_{-1}^{1} p_{n-1}(x) P_m(x)\,dx = 0, \tag{54}$$

and so

$$\left| \int_{-1}^{1} \varphi(x) P_m(x)\,dx \right| \leq |\mu|([-c,c]) \max_{\xi \in [-c,c]} \left| \int_{-1}^{1} \exp(i\xi x) x^n P_m(x)\,dx \right|. \tag{55}$$

We now observe that

$$x^n P_m(x) = \sum_{k=m-n}^{m+n} b_k P_k(x), \tag{56}$$

where

$$b_k = \sqrt{k+\frac{1}{2}} \int_{-1}^{1} x^n P_m(x) P_k(x)\,dx. \tag{57}$$

By combining (56) and Lemma 3, we see that

$$\begin{aligned}\left| \int_{-1}^{1} \exp(i\xi x) x^n P_m(x)\,dx \right| &\leq \sum_{k=m-n}^{m+n} \frac{2\,|b_k| \left|\frac{\xi}{2}\right|^k}{\Gamma(k+1)} \\ &\leq \frac{(4n+2)\max\{|b_k|\}\,\left(\frac{c}{2}\right)^{m+n}}{\Gamma(m-n+1)},\end{aligned} \tag{58}$$

for all $|\xi| \leq c$. Together with (55), this gives us (52). □

Remark 1. *Using the well-known approximation*

$$j_\nu(z) \approx \frac{1}{z\sqrt{2e}} \left(\frac{ez}{2(\nu + \frac{1}{2})} \right)^{\nu+1} = \left(\frac{e}{2\sqrt{2e}(\nu + \frac{1}{2})} \right) \left(\frac{ez}{2(\nu + \frac{1}{2})} \right)^{\nu} \tag{59}$$

in lieu of the rather crude bound (50), we see that

$$\begin{aligned} &\left| \int_{-1}^{1} \exp(i\xi x) x^n P_m(x)\, dx \right| \\ &= \left| \sum_{k=m-n}^{m+n} 2i^k b_k j_k(\xi) \right| \\ &\leq (4n+2) \max\{|b_k|\} \sum_{k=m-n}^{m+n} |j_k(\xi)| \\ &\approx (4n+2) \max\{|b_k|\} \sum_{k=m-n}^{m+n} \left(\frac{e}{2\sqrt{2e}(k + \frac{1}{2})} \right) \left(\frac{ec}{2(k + \frac{1}{2})} \right)^{k}, \end{aligned} \tag{60}$$

for all $|\xi| \leq c$. *When* $m > ec/2 + n - \frac{1}{2}$,

$$\left(\frac{ec}{2(k + \frac{1}{2})} \right) < 1 \tag{61}$$

and the preceding sum is bounded by a multiple of

$$\frac{2n}{m - n + \frac{1}{2}} \left(\frac{ec}{2\left(m - n + \frac{1}{2}\right)} \right)^{m-n}. \tag{62}$$

So we expect the coefficients in the Legendre expansion of φ *to decay superexponentially as soon as this condition is met.*

2.5 Truncated singular value decompositions

If $\mathscr{A}$ is a complex-valued $m \times n$ matrix with $m \geq n$, then any decomposition of the form

$$\mathscr{A} = \begin{pmatrix} \mathbf{u_1} & \mathbf{u_2} & \cdots & \mathbf{u_m} \end{pmatrix} \begin{pmatrix} \sigma_1 & & & \\ & \sigma_2 & & \\ & & \ddots & \\ & & & \sigma_n \\ 0 & 0 & \cdots & 0 \\ \vdots & \vdots & \ddots & \vdots \\ 0 & 0 & \cdots & 0 \end{pmatrix} \begin{pmatrix} \mathbf{v_1} & \mathbf{v_2} & \cdots & \mathbf{v_n} \end{pmatrix}^*, \tag{63}$$

where $\sigma_1, \ldots, \sigma_n \in \mathbb{R}$, $\{\mathbf{u_1}, \ldots, \mathbf{u_m}\}$ is an orthonormal basis in $\mathbb{C}^m$ and $\{\mathbf{v_1}, \ldots, \mathbf{v_n}\}$ is an orthonormal basis in $\mathbb{C}^n$, is known as a singular value decomposition of $\mathscr{A}$. The quantities $\sigma_1, \ldots, \sigma_n$ are uniquely determined up to

ordering, and they are known as the singular values of $\mathscr{A}$. It is conventional to arrange them in descending order, and we will assume that this is the case with all singular value decompositions that we consider.

A k-truncated singular value decomposition of $\mathscr{A}$ is an approximation of the form

$$\mathscr{A} \approx \begin{pmatrix} \mathbf{u_1} & \mathbf{u_2} & \cdots & \mathbf{u_k} \end{pmatrix} \begin{pmatrix} \sigma_1 & & & \\ & \sigma_2 & & \\ & & \ddots & \\ & & & \sigma_k \end{pmatrix} \begin{pmatrix} \mathbf{v_1} & \mathbf{v_2} & \cdots & \mathbf{v_k} \end{pmatrix}^*, \tag{64}$$

where (63) is a singular value decomposition of $\mathscr{A}$ with $\sigma_1 \geq \sigma_2 \geq \cdots \geq \sigma_n$ and $1 \leq k \leq n$. Typically, some desired precision $\epsilon > 0$ is specified and k is taken to be the least integer between 1 and $n-1$ such that $\sigma_{k+1} < \epsilon$, if such an integer exists, or $k = n$ otherwise. In this case, we say that (64) is a singular value decomposition which has been truncated at precision ϵ. We call the vector

$$\mathbf{x} = \begin{pmatrix} \mathbf{v_1} & \mathbf{v_2} & \cdots & \mathbf{v_k} \end{pmatrix} \begin{pmatrix} \frac{1}{\sigma_1} & & & \\ & \frac{1}{\sigma_2} & & \\ & & \ddots & \\ & & & \frac{1}{\sigma_k} \end{pmatrix} \begin{pmatrix} \mathbf{u_1} & \mathbf{u_2} & \cdots & \mathbf{u_k} \end{pmatrix}^* \mathbf{y} \tag{65}$$

the solution of the linear system $\mathscr{A}\mathbf{x} = \mathbf{y}$ obtained from the truncated singular value decomposition (64).

The following theorem implies that, when a linear system admits an approximate solution with a modest norm, and it is solved numerically using a truncated singular value decomposition, the computed solution will have both a small residual and a modest norm. The proof can be found in [23].

Theorem 3 *Suppose that $\mathscr{A} \in \mathbb{C}^{m\times n}$, where $m \geq n$, and let $\sigma_1 \geq \sigma_2 \geq \cdots \geq \sigma_n$ be the singular values of $\mathscr{A}$. Let $\mathbf{b} \in \mathbb{C}^m$, and suppose that $\mathbf{x} \in \mathbb{C}^n$ satisfies*

$$\mathscr{A}\mathbf{x} = \mathbf{b}. \tag{66}$$

Let $\epsilon > 0$, and suppose further that

$$\widehat{\mathbf{x}}_k = (\mathscr{A} + \mathscr{E})_k^\dagger (\mathbf{b} + \mathbf{e}), \tag{67}$$

where $(\mathscr{A} + \mathscr{E})_k^\dagger$ is the pseudo-inverse of a k-truncated singular value decomposition of $\mathscr{A} + \mathscr{E}$, so that

$$\widehat{\sigma}_k \geq \epsilon \geq \widehat{\sigma}_{k+1}, \tag{68}$$

where $\widehat{\sigma}_k$ and $\widehat{\sigma}_{k+1}$ are the kth and $(k+1)$th largest singular values of $\mathscr{A} + \mathscr{E}$, and where $\mathscr{E} \in \mathbb{C}^{m\times n}$ and $\mathbf{e} \in \mathbb{C}^m$, with $\|\mathscr{E}\|_2 < \epsilon/2$. Then

$$\|\widehat{\mathbf{x}}_k\|_2 \leq \frac{1}{\widehat{\sigma}_k}(2\epsilon\|\mathbf{x}\|_2 + \|\mathbf{e}\|_2) + \|\mathbf{x}\|_2. \tag{69}$$

and

$$\|\mathscr{A}\widehat{\mathbf{x}}_k - \mathbf{b}\|_2 \leq 5\epsilon\|\mathbf{x}\|_2 + \frac{3}{2}\|\mathbf{e}\|_2. \tag{70}$$

We will make use of the following simplified version of this theorem.

Corollary 2 *Suppose that* $\mathscr{A} \in \mathbb{C}^{m\times n}$*, where* $m \geq n$*, and let* $\sigma_1 \geq \sigma_2 \geq \cdots \geq \sigma_n$ *be the singular values of* $\mathscr{A}$*. Let* $\epsilon > 0$ *and* $\mathbf{b} \in \mathbb{C}^n$*, and suppose that* $\boldsymbol{\delta}\mathbf{b} \in \mathbb{C}^n$ *and* $\mathbf{x} \in \mathbb{C}^n$ *satisfy*

$$\mathscr{A}\mathbf{x} = \mathbf{b} + \boldsymbol{\delta}\mathbf{b}, \tag{71}$$

where $\boldsymbol{\delta}\mathbf{b} \lesssim \epsilon\|\mathscr{A}\|_2\|\mathbf{x}\|_2$*. Suppose that*

$$\widehat{\mathbf{x}}_k = (\mathscr{A} + \mathscr{E})_k^{\dagger}(\mathbf{b} + \mathbf{e}), \tag{72}$$

where $(\mathscr{A} + \mathscr{E})_k^{\dagger}$ *is the pseudo-inverse of a* k*-truncated singular value decomposition of* $\mathscr{A} + \mathscr{E}$*, so that*

$$\widehat{\sigma}_k \geq \epsilon\|\mathscr{A}\|_2 \geq \widehat{\sigma}_{k+1}, \tag{73}$$

where $\widehat{\sigma}_k$ *and* $\widehat{\sigma}_{k+1}$ *are the* k*th and* $(k+1)$*th largest singular values of* $\mathscr{A} + \mathscr{E}$*, and where* $\mathscr{E} \in \mathbb{C}^{m\times n}$ *and* $\mathbf{e} \in \mathbb{C}^m$*, with* $\|\mathscr{E}\|_2 < \epsilon\|\mathscr{A}\|_2/2$ *and* $\|\mathbf{e}\|_2 \lesssim \epsilon\|\mathbf{b}\|_2$*. Then*

$$\|\widehat{\mathbf{x}}_k\|_2 \lesssim \|\mathbf{x}\|_2 \tag{74}$$

and

$$\|\mathscr{A}\widehat{\mathbf{x}}_k - \mathbf{b}\|_2 \lesssim \epsilon\|\mathscr{A}\|_2\|\mathbf{x}\|_2. \tag{75}$$

3 Analysis of the Levin equation

This section contains our analysis of the Levin equation. The two principal results are Theorems 4 and 5. Theorem 4 generalizes the classical result of [1] by showing that, whenever g' is nonzero over the interval and the ratio of the maximum absolute value of g' to the minimum absolute value of g' is small, the Levin equation admits a well-behaved solution which can be approximated by a polynomial expansion at a cost which is independent of the magnitude of g'. Theorem 5 shows that, on an interval in which g' is of small magnitude, the Levin equation admits a well-behaved solution which can be represented by a polynomial expansion at a cost which decreases with the magnitude of g'. It applies whether or not g' has zeros in the interval. We begin with the following lemma, which applies in the simple case when g' is equal to a nonzero constant W.

Lemma 4 *Suppose that* $f : [-1, 1] \to \mathbb{C}$ *admits an infinitely differentiable extension to a neighborhood of* $[-1, 1]$ *and* $W \neq 0$*. Suppose further that* $0 < \epsilon < 1$*, and let* $W_0 = c_f(\epsilon)$*, where* $c_f(\epsilon)$ *is defined in Definition 1. Then there exists an entire function* $p_b \in S'(\mathbb{R})$ *and a constant* $C(W_0)$ *depending only on* W_0 *such that*

1. $\widehat{p_b}$ *is a tempered distribution of order one supported on* $[-W_0, W_0]$*,*
2. $|p_b'(x) + iWp_b(x) - f(x)| \leq \epsilon\|f\|_{L^\infty([-1,1])}$ *for all* $x \in [-1, 1]$*,*
3. $\|p_b\|_{L^\infty([-1,1])} \leq C(W_0)\min\left\{1, \dfrac{1}{|W|}\right\}\|f\|_{L^\infty([-1,1])}$ *and*

4. $\|p_b'\|_{L^\infty([-1,1])} \le C(W_0) \min\left\{1, \dfrac{1}{|W|}\right\} \|f\|_{L^\infty([-1,1])}$.

Proof We let $f_b \in S(\mathbb{R})$ be a function with bandlimit $W_0 = c_f(\epsilon)$ such that conditions (1)-(4) in Definition 1 hold, and define the function p_b via the formula

$$p_b(x) = \text{p.v.} \int_{-W_0}^{W_0} \frac{\widehat{f}_b(\xi)}{i(W+\xi)} \exp(i\xi x)\, d\xi. \tag{76}$$

That is, p_b is the inverse Fourier transform of the product of the tempered distribution $\mathcal{T}_W$ defined via

$$\langle \mathcal{T}_W, \varphi \rangle = \text{p.v.} \int_{-\infty}^{\infty} \frac{\varphi(\xi)}{i\,(W+\xi)}\, d\xi \tag{77}$$

and the infinitely differentiable function $\widehat{f_b}$. It is clear that $\widehat{p_b}$ is a tempered distribution of order one which is supported on $[-W_0, W_0]$, so the first of the conditions listed above is satisfied; in particular, p_b is an entire function by a the Schwartz-Paley-Wiener theorem.

Since

$$p_b'(x) + iWp_b(x) = \int_{-W_0}^{W_0} \frac{i\,(W+\xi)\,\widehat{f}_b(\xi)}{i(W+\xi)} \exp(i\xi x)\, d\xi = f_b(x) \tag{78}$$

and

$$\|f - f_b\|_{L^\infty([-1,1])} \le \epsilon \|f\|_{L^\infty([-1,1])}, \tag{79}$$

the second of the properties of p_b listed above holds.

To establish the third of the properties of p_b listed above, we first assume that $|W| \le W_0 + 1$. Then we have

$$\begin{aligned} p_b(x) &= \text{p.v.} \int_{-W_0}^{W_0} \frac{\widehat{f}_b(\xi)}{i(W+\xi)} \exp(ix\xi)\, d\xi \\ &= \text{p.v.} \int_{-W-2W_0-1}^{-W+2W_0+1} \frac{\widehat{f}_b(\xi)}{i(W+\xi)} \exp(ix\xi)\, d\xi \\ &= \int_{-W-2W_0-1}^{-W+2W_0+1} \frac{\widehat{f}_b(\xi)\exp(ix\xi) - \widehat{f}_b(-W)\exp(-ixW)}{i(W+\xi)}\, d\xi \end{aligned} \tag{80}$$

for all $x \in \mathbb{R}$, where the last equality follows from the fact that $1/(W+\xi)$ is odd about $\xi = -W$. By the mean value theorem, there exists a function $\eta(\xi)$ such that

$$p_b(x) = \int_{-W-2W_0-1}^{-W+2W_0+1} \frac{G'(\eta(\xi))(W+\xi)}{i(W+\xi)}\, d\xi = -i \int_{-W-2W_0-1}^{-W+2W_0+1} G'(\eta(\xi))\, d\xi \tag{81}$$

for all $x \in \mathbb{R}$, where

$$G(\xi) = \widehat{f}_b(\xi) \exp(ix\xi). \tag{82}$$

Since

$$G'(\xi) = \widehat{f}_b{}'(\xi) \exp(ix\xi) + ix\widehat{f}_b(\xi) \exp(ix\xi), \tag{83}$$

we have

$$|p_b(x)| \le 2(2W_0+1) \left(\left\| \widehat{f}_b{}' \right\|_{L^\infty(\mathbb{R})} + \left\| \widehat{f}_b \right\|_{L^\infty(\mathbb{R})} \right) \tag{84}$$

for all $x \in [-1,1]$ (note that we are now only considering x in $[-1,1]$). Now making use of properties (3) and (4) in Definition 1 gives us

$$\|p_b\|_{L^\infty([-1,1])} \leq 16(2W_0+1)\,\|f\|_{L^\infty([-1,1])}\,. \tag{85}$$

An analogous argument which makes use of the fact that

$$p_b'(x) = \int_{-W-2W_0-1}^{-W+2W_0+1} \frac{H(\xi)-H(-W)}{i(W+\xi)}\,d\xi, \tag{86}$$

where

$$H(\xi) = i\xi\widehat{f}_b(\xi)\exp(ix\xi), \tag{87}$$

shows that

$$\begin{aligned}\left\|p_b'\right\|_{L^\infty([-1,1])} &\leq 8(2W_0+1)\,(1+2(|W|+2W_0+1))\,\|f\|_{L^\infty([-1,1])}\\ &\leq 8\,(2W_0+1)\,(6W_0+5)\,\|f\|_{L^\infty([-1,1])}\end{aligned} \tag{88}$$

when $|W| \leq W_0+1$.

We now suppose that $|W| > W_0+1$. Then

$$|p_b(x)| = \left|\int_{-W_0}^{W_0} \frac{\widehat{f}_b(\xi)\exp(i\xi x)}{i(W+\xi)}\,d\xi\right| \leq \frac{2W_0}{|W|-|W_0|}\left\|\widehat{f}_b\right\|_{L^\infty(\mathbb{R})} \tag{89}$$

and

$$|p_b'(x)| = \left|\int_{-W_0}^{W_0} \frac{\widehat{f}_b(\xi)\exp(i\xi x)i\xi}{i(W+\xi)}\,d\xi\right| \leq \frac{W_0^2}{|W|-|W_0|}\left\|\widehat{f}_b\right\|_{L^\infty(\mathbb{R})} \tag{90}$$

hold for all $x \in \mathbb{R}$. From the above inequalities, the fact that

$$\frac{1}{|W|-W_0} \leq \frac{W_0+1}{|W|} \tag{91}$$

and property (3) in Definition 1, we see that

$$\|p_b\|_{L^\infty(\mathbb{R})} \leq \frac{8W_0(W_0+1)}{|W|}\,\|f\|_{L^\infty([-1,1])} \tag{92}$$

and

$$\left\|p_b'\right\|_{L^\infty(\mathbb{R})} \leq \frac{4W_0^2(W_0+1)}{|W|}\,\|f\|_{L^\infty([-1,1])} \tag{93}$$

whenever $|W| > W_0+1$. The third of the conditions on p_b listed in the conclusion of the lemma follows from the combination of (85) and (92), while the fourth is obtained by combining (88) and (93). □

In accordance with Remark 1, the sequence $\{a_m\}$ of Legendre coefficients of the approximate solution p_b of the Levin equation appearing in Lemma 4 decays superexponentially once $m > e/2c_f(\epsilon) + 1/2$. Consequently, p_b can be represented to a fixed relative precision via a polynomial expansion at a cost which depends on the complexity of f but not the magnitude of W.

We now move on to the case in which g' is nonconstant, but with no zeros on the interval $[-1,1]$. To that end, we suppose that $f : [-1,1] \to \mathbb{C}$ and $g : [-1,1] \to \mathbb{R}$ admit infinitely differentiable extensions to a neighborhood of

$[-1,1]$, and that the extension of g' is nonzero in an open interval containing $[-1,1]$. We also let

$$G_0 = \min_{-1\le x\le 1} |g'(x)|, \quad W = \frac{1}{2}\int_{-1}^{1} g'(x)\,dx \tag{94}$$

and define $u : [-1,1] \to [-1,1]$ via the formula

$$u(x) = -1 + \frac{1}{W}\int_{-1}^{x} g'(y)\,dy. \tag{95}$$

Because g' is nonzero in a neighborhood of $[-1,1]$, u is invertible and its inverse extends to an open neighborhood of $[-1,1]$. Finally, we define $h : [-1,1] \to [-1,1]$ via the formula

$$h(z) = \frac{f\left(u^{-1}(z)\right)}{u'\left(u^{-1}(z)\right)} = f\left(u^{-1}(z)\right)\frac{du^{-1}}{dz}(z). \tag{96}$$

Note that u is independent of the magnitude of g', in the sense that it is the same for any rescaling of g' by a nonzero constant. The function h is independent of the magnitude of g' in the same sense.

With the preceding notations and assumptions, we have the following:

Theorem 4 *Suppose that $0 < \epsilon < 1$, and let $W_0 = c_h(\epsilon)$, where $c_h(\epsilon)$ is defined in Definition 1. Then there exists a constant $C(W_0)$, depending only on W_0, and an infinitely differentiable function $p_b : [-1,1] \to \mathbb{C}$ such that*

1. *the Fourier transform of $p_b\left(u^{-1}(z)\right)$ is a tempered distribution of order 1 supported on the interval $[-W_0, W_0]$,*
2. $|p_b'(x) + ig'(x)p_b(x) - f(x)| \le \epsilon\dfrac{|W|}{G_0}\|f\|_{L^\infty([-1,1])}$ *for all $x \in [-1,1]$,*
3. $\|p_b\|_{L^\infty([-1,1])} \le C(W_0)\dfrac{|W|}{G_0}\min\left\{1, \dfrac{1}{|W|}\right\}\|f\|_{L^\infty([-1,1])}$ *and*
4. $\|p_b'\|_{L^\infty([-1,1])} \le C(W_0)\dfrac{|W|}{G_0}\min\left\{1, \dfrac{1}{|W|}\right\}\|f\|_{L^\infty([-1,1])}$.

Proof By introducing the new variable $z = u(x)$, we transform the Levin equation

$$p'(x) + ig'(x)p(x) = f(x), \qquad -1 < x < 1, \tag{97}$$

into the simplified form

$$p'(z) + iWp(z) = h(z), \qquad -1 < z < 1. \tag{98}$$

Our assumptions on f and g, and the method we used to construct u ensure that h admits an infinitely differentiable extension to a neighborhood of $[-1,1]$. Applying Lemma 4 to (98) shows that, for all $0 < \epsilon < 1$, there exists an entire function p_1 such that

1. $\widehat{p_1}$ is a tempered distribution of order 1 supported on the interval $[-W_0, W_0]$,

2. $|p_1'(z) + iWp_1(z) - h(z)| \leq \epsilon \|h\|_{L^\infty([-1,1])}$ for all $z \in [-1,1]$,
3. $\|p_1\|_{L^\infty([-1,1])} \leq C(W_0) \min\left\{1, \frac{1}{|W|}\right\} \|h\|_{L^\infty([-1,1])}$ and
4. $\|p_1'\|_{L^\infty([-1,1])} \leq C(W_0) \min\left\{1, \frac{1}{|W|}\right\} \|h\|_{L^\infty([-1,1])}$.

We now define p_b via the formula $p_b(x) = p_1(u(x))$. It is clear that the first condition on p_b listed above is satisfied. We observe that, since $g'(x) = Wu'(x)$,

$$\|h\|_{L^\infty([-1,1])} \leq \frac{|W|}{G_0} \|f\|_{L^\infty([-1,1])}. \tag{99}$$

Combining (99) and properties of p_1 listed above yields

$$\|p_b\|_{L^\infty([-1,1])} \leq C(W_0) \frac{|W|}{G_0} \min\left\{1, \frac{1}{|W|}\right\} \|f\|_{L^\infty([-1,1])}, \tag{100}$$

$$\|p_b'\|_{L^\infty([-1,1])} \leq C(W_0) \frac{|W|}{G_0} \min\left\{1, \frac{1}{|W|}\right\} \|f\|_{L^\infty([-1,1])} \tag{101}$$

and

$$|p_b(x) - ig'(x)p_b(x) - f(x)| \leq \epsilon \frac{|W|}{G_0} \|f\|_{L^\infty([-1,1])}, \tag{102}$$

the latter of which holds for all $x \in [-1,1]$. This suffices to establish the theorem. □

We emphasize that Theorem 4 does not imply that the approximate solution p_b of the Levin equation has a Fourier transform which is a tempered distribution with compact support. Instead, we have

$$p_b(x) = \langle \widehat{p_1}, \eta_x \rangle \quad \text{with} \quad \eta_x(\xi) = \exp(iu(x)\xi), \tag{103}$$

where $\widehat{p_1}$ is a tempered distribution of order one with compact support $[-W_0, W_0]$, where $W_0 = c_h(\epsilon)$ is independent of the magnitude of g'. Since p_b is the composition of a bandlimited function p_1, whose bandlimit does not depend on the magnitude of g', and the function u, which is analytic on an open neighborhood of $[-1,1]$ and which is also independent of the magnitude of g', it follows that p_b is an analytic function on an open neighborhood of $[-1,1]$, whose smoothness is characterized independently of the magnitude of g'. The coefficients $\{a_m\}$ in its Legendre expansion decay faster than m^{-k} for any positive integer k; moreover, p_b can be approximated to a fixed relative precision via a Legendre expansion at a cost which does not depend on the magnitude of g', but which does depend on the complexity of h and u.

It would be of interest to develop better estimates on the rate of decay of the Legendre coefficients of p_b, as we did in the case when g' is constant, but useful results of this type seem to be fairly complicated. Indeed, the difficulty in estimating the complexity of p_b *a priori* is one of the principal motivations for the adaptive version of the Levin algorithm that we introduce in this article.

We close this section with the following theorem which shows that, if g' is of small magnitude, then the Levin equation admits a solution which can be well-approximated by a bounded, bandlimited function p_b.

Theorem 5 *Suppose that $f : [-1,1] \to \mathbb{C}$ and $g : [-1,1] \to \mathbb{R}$ admit extensions to infinitely differentiable functions in a neighborhood of $[-1,1]$, and that*

$$G_1 = \max_{-1 \le x \le 1} |g'(x)| < \frac{1}{2}. \tag{104}$$

Let $0 < \epsilon < 1$ be given, and define the integer n via the formula

$$n = \left\lfloor \frac{\log(\epsilon)}{\log(2G_1)} \right\rfloor. \tag{105}$$

Then there exists an infinitely differentiable function $p_b \in S'(\mathbb{R})$ such that

1. *$\widehat{p_b}$ is a tempered distribution of order 1 supported on the interval*
$$[-c_f(\epsilon) - nc_{g'}(\epsilon), c_f(\epsilon) + nc_{g'}(\epsilon)], \tag{106}$$
where $c_f(\epsilon)$ and $c_{g'}(\epsilon)$ are defined in Definition 1,
2. *$|p_b'(x) + ig'(x)p_b(x) - f(x)| \le 2\epsilon \left(1 + \dfrac{G_1}{1-2G_1}\right) \|f\|_{L^\infty([-1,1])}$ for all $x \in [-1,1]$,*
3. *$\|p_b\|_{L^\infty([-1,1])} \le \dfrac{2}{1-2G_1} \|f\|_{L^\infty([-1,1])}$ and*
4. *$\|p_b'\|_{L^\infty([-1,1])} \le 4\left(1 + \dfrac{G_1}{1-2G_1}\right) \|f\|_{L^\infty([-1,1])}$.*

Proof We let f_b and g_b' be bandlimited approximates of f and g' which satisfy conditions (1)-(4) in Definition 1. We next define $A : L^\infty([-1,1]) \to L^\infty([-1,1])$ via the formula

$$A[\varphi](x) = -i \int_0^x g_b'(y)\varphi(y)\, dy. \tag{107}$$

Obviously, $\|A\|_\infty$ is bounded by $\|g_b'\|_{L^\infty([-1,1])}$, which is less than $(1+\epsilon)G_1 \le 2G_1 < 1$ by property (1) in Definition 1. Now we let $G_2 = (1+\epsilon)G_1$,

$$h(x) = \int_0^x f_b(y)\, dy \tag{108}$$

and

$$p_b(x) = \sum_{k=0}^{n} A^k[h](x), \tag{109}$$

where A^k denotes the repeated application of the operator A and n is defined by (105). Since $\|f_b\|_{L^\infty([-1,1])} \le (1+\epsilon)\|f\|_{L^\infty([-1,1])}$ by property (1) in Definition 1, we have

$$\begin{aligned} \|p_b\|_{L^\infty([-1,1])} &\le \left(\sum_{k=0}^{n} \|A\|_\infty^k\right) \|h\|_{L^\infty([-1,1])} \\ &\le \frac{1+G_2^{n+1}}{1-G_2} \|f\|_{L^\infty([-1,1])} \\ &\le \frac{1+\epsilon}{1-G_2} \|f\|_{L^\infty([-1,1])}, \end{aligned} \tag{110}$$

which implies the third property of p_b listed above. Since $h'(x) = f_b(x)$ and

$$\frac{d}{dx} A^k [h](x) = -ig_b'(x) A^{k-1} [h](x), \tag{111}$$

we have

$$\begin{aligned} p_b'(x) &= f_b(x) - ig_b'(x) \sum_{k=0}^{n-1} A^k [h](x) \\ &= f_b(x) - ig_b'(x) \sum_{k=0}^{n} A^k [h](x) + ig_b'(x) A^n [h](x) \\ &= f_b(x) - ig_b'(x) p_b(x) + ig_b'(x) A^n [h](x) \end{aligned} \tag{112}$$

for all $x \in [-1,1]$. From this and (110), we see that

$$\begin{aligned} \left\| p_b'(x) \right\|_{L^\infty([-1,1])} &\leq \|f_b\|_{L^\infty([-1,1])} + \left\| g' \right\|_{L^\infty([-1,1])} \|p_b\|_{L^\infty([-1,1])} \\ &\quad + G_2^{n+1} \|f_b\|_{L^\infty([-1,1])} \\ &\leq \left((1+\epsilon) + G_1 \frac{1+\epsilon}{1-G_2} + \epsilon(1+\epsilon) \right) \|f\|_{L^\infty([-1,1])} \\ &\leq \left((1+\epsilon)^2 + \frac{2G_1}{1-G_2} \right) \|f\|_{L^\infty([-1,1])}, \end{aligned} \tag{113}$$

from which the fourth of the properties of p_b listed in the conclusion of the theorem follows. Similarly, (112) implies that

$$\begin{aligned} \left| p_b'(x) + ig_b'(x) p_b(x) - f(x) \right| &\leq \left| p_b'(x) + ig_b'(x) p_b(x) - f_b(x) \right| + |f_b(x) - f(x)| \\ &\leq \left| ig_b'(x) A^n [h](x) \right| + |f_b(x) - f(x)| \\ &\leq G_2^{n+1} \|f\|_{L^\infty([-1,1])} + \epsilon \|f\|_{L^\infty([-1,1])} \\ &\leq 2\epsilon \|f\|_{L^\infty([-1,1])} \end{aligned} \tag{114}$$

for all $x \in [-1,1]$. Combining (114) with (110), (113) and using the properties of the approximates f_b and g_b, we see that

$$\begin{aligned} &\left| p_b'(x) + ig'(x) p_b(x) - f(x) \right| \\ \leq &\left| p_b'(x) + ig_b'(x) p_b(x) - f(x) \right| + \left| ig'(x) p_b(x) - ig_b'(x) p_b(x) \right| \\ \leq &2\epsilon \|f\|_{L^\infty([-1,1])} + \|p_b\|_{L^\infty([-1,1])} \left\| g' - g_b' \right\|_{L^\infty([-1,1])} \\ \leq &\left(2 + \left(\frac{1+\epsilon}{1-G_2} \right) \left(\left\| g' \right\|_{L^\infty([-1,1])} \right) \right) \epsilon \|f\|_{L^\infty([-1,1])} \end{aligned} \tag{115}$$

for all $x \in [-1,1]$. The second of the properties of p_b listed above follows from (115).

It remains only to establish the first of the properties of p_b listed above. To do so, we first observe that the Fourier transform of h is

$$\text{p.v.} \frac{\widehat{f_b}(\xi)}{i\xi} + \frac{1}{2}\delta(\xi) \left(\int_0^\infty f_b(x)\, dx - \int_{-\infty}^0 f_b(x)\, dx, \right), \tag{116}$$

which is a tempered distribution of order one supported on the interval $[-c_\epsilon(f), c_\epsilon(f)]$. Next, we suppose that ψ is a $C^\infty(\mathbb{R})$ function whose Fourier transform is a tempered distribution of order 1 supported on $[-c, c]$. The Fourier transform of ψ times the function $g_b' \in S(\mathbb{R})$ is a tempered distribution of order 0 supported on $\left[-c - c_{g'}(\epsilon), c + c_{g'}(\epsilon)\right]$. Since $A[\psi]$ is obtained by integrating this convolution, its Fourier transform is a tempered distribution of order

1 with bandlimit $\left[-c - c_{g'}(\epsilon), c + c_{g'}(\epsilon)\right]$. It now follows by induction that the Fourier transform of $A^k[h]$ is a tempered distribution of order 1 with bandlimit $\left[-c_f(\epsilon) - kc_{g'}(\epsilon), c_f(\epsilon) + kc_{g'}(\epsilon)\right]$. Combining this with (109) yields the first property of p_b listed above. □

The bandlimit of the function p_b whose existence is established in Theorem 5 decreases with magnitude of g'. Consequently, on any interval on which g' is sufficiently small, we expect to be able to represent p_b to a fixed relative accuracy with a polynomial expansion whose number of terms is bounded. Moreover, this is the case whether or not g' has zeros in the interval.

4 Numerical aspects of the Levin method

In this section, we show that high-accuracy can be obtained when the Levin equation (2) is discretized via a Chebyshev spectral collocation method and the resulting linear system is solved with a truncated singular value decomposition, regardless of the magnitude of g' and whether or not it has zeros. There is one unusual feature of the spectral collocation method we consider, namely, we use the k-point extremal Chebyshev grid to represent the unknown solution p of the system, but we require that the Levin equation hold on the nodes of the $2k$-point extremal Chebyshev grid. We take this approach because, while we approximate both g' and p by polynomials of degree k, the Levin equation involves the product of g' and p, which is approximated by a polynomial of degree $2k$. We note, however, that while our rigorous bounds depend on imposing conditions at $2k$ points, in practice there is little harm in forming a square system (i.e., in imposing conditions only at k points). Indeed, we explain in the beginning of the next section why the imposition of k conditions almost always suffices.

In this section, we use the symbol $\widehat{x}$ to mean the computed approximation to x, rather than the Fourier transform of x.

Throughout this section, we will assume that $f : [-1, 1] \to \mathbb{C}$ and $g : [-1, 1] \to \mathbb{R}$ admit continuously differentiable extensions to a neighborhood of $[-1, 1]$, and that $0 < \epsilon < 1$. Moreover, we let

$$G_0 = \min_{-1 \le x \le 1} |g'(x)|, \quad G_1 = \max_{-1 \le x \le 1} |g'(x)| \quad \text{and} \quad W = \frac{1}{2} \int_{-1}^{1} g'(x)\, dx. \tag{117}$$

We consider separately the case when $G_0 > 0$ and the case when $G_1 < 1/4$, and provide error bounds on the absolute error $|\widehat{I} - I|$ of the Levin method for evaluating an integral I of the form (1), using Chebyshev collocation points and the truncated singular value decomposition, applied to the Levin equation over a single interval $[-1, 1]$. The main results of this section are given by inequality (153) for the case $G_0 > 0$, and by inequality (164) for the case $G_1 < 1/4$.

4.1 The case when $G_0 > 0$

We first consider the case in which $G_0 > 0$. Letting $W_0 = c_h(\epsilon)$, where $c_h(\epsilon)$ is defined in Definition 1 and h is defined via the formula (96), we invoke Theorem 4 to see that there exist a function p_b which is analytic on a neighborhood on $[-1,1]$ and whose smoothness is characterized independently of the magnitude g', and a constant $C(W_0)$ depending only on W_0 such that

$$|p_b'(x) + ig'(x)p_b(x) - f(x)| \leq \epsilon \frac{|W|}{G_0} \|f\|_{L^\infty([-1,1])} \quad \text{for all} \quad x \in [-1,1], \tag{118}$$

$$\|p_b\|_{L^\infty([-1,1])} \leq C(W_0) \frac{|W|}{G_0} \min\left\{1, \frac{1}{|W|}\right\} \|f\|_{L^\infty([-1,1])} \tag{119}$$

and

$$\|p_b'\|_{L^\infty([-1,1])} \leq C(W_0) \frac{|W|}{G_0} \min\left\{1, \frac{1}{|W|}\right\} \|f\|_{L^\infty([-1,1])}. \tag{120}$$

Recalling that h is the same for any rescaling of g' by a nonzero constant, we note that W_0 is independent of the magnitude of g'. Moreover, it is clear from the discussion following Theorem 4 that

$$p_b(x) = \sum_{n=0}^{\infty} a_n T_n(x), \tag{121}$$

where $|a_n|$ is bounded by a rapidly decaying function of n which is independent of the magnitude of g'.

We claim that there is an integer k such that

$$\begin{aligned} &\left\| \mathsf{P}_k\left[p_b\right]' + i\mathsf{P}_k\left[g'\right]\mathsf{P}_k\left[p_b\right] - \left(p_b' + ig'p_b\right)\right\|_{L^\infty([-1,1])} \\ &\leq \epsilon \|p_b'\|_{L^\infty([-1,1])} + 4\epsilon G_1 \|p_b\|_{L^\infty([-1,1])} \\ &\leq \epsilon\left(1 + 4G_1\right) C(W_0) \frac{|W|}{G_0} \min\left\{1, \frac{1}{|W|}\right\} \|f\|_{L^\infty([-1,1])} \end{aligned} \tag{122}$$

holds regardless of the magnitude of g'; that is, k can be chosen independent of the magnitude of g'. It will be important in what follows to note that while we are approximating p_b and g' with polynomials of degree k, the function $\mathsf{P}_k\left[p_b\right]' + i\mathsf{P}_k\left[g'\right]\mathsf{P}_k\left[p_b\right]$ is a polynomial of degree $2k$. To see that (122) holds, we first observe that (121) together with Formulas (28) and (29) in Subsection 2.2 imply that we can choose k independently of the magnitude of g' such that

$$\left\|\mathsf{P}_k\left[p_b\right] - p_b\right\|_{L^\infty([-1,1])} \leq \epsilon \left\|p_b\right\|_{L^\infty([-1,1])} \tag{123}$$

and

$$\left\|\mathsf{P}_k\left[p_b\right]' - p_b'\right\|_{L^\infty([-1,1])} \leq \epsilon \left\|p_b'\right\|_{L^\infty([-1,1])}. \tag{124}$$

Clearly, we can also choose k independently of the magnitude of g' to ensure that

$$\left\|\mathsf{P}_k\left[g'\right]-g'\right\|_{L^\infty([-1,1])}\leq\epsilon\left\|g'\right\|_{L^\infty([-1,1])}, \tag{125}$$

since g is assumed to be slowly varying, and

$$\left\|\mathsf{P}_{2k}\left[f\right]-f\right\|_{L^\infty([-1,1])}\leq\epsilon\left\|f\right\|_{L^\infty([-1,1])}. \tag{126}$$

Now (123) and (125) together with the assumption that $0<\epsilon<1$ imply

$$\left\|\mathsf{P}_k[p_b]\right\|_{L^\infty([-1,1])}\leq 2\left\|p_b\right\|_{L^\infty([-1,1])} \tag{127}$$

and

$$\left\|\mathsf{P}_k[g']\right\|_{L^\infty([-1,1])}\leq 2\left\|g'\right\|_{L^\infty([-1,1])}. \tag{128}$$

It follows readily that

$$\begin{aligned}
&\left\|\mathsf{P}_k\left[g'\right]\mathsf{P}_k\left[p_b\right]-g'p_b\right\|_{L^\infty([-1,1])}\\
\leq&\left\|\mathsf{P}_k\left[p_b\right]\right\|_{L^\infty([-1,1])}\left\|\mathsf{P}_k\left[g'\right]-g'\right\|_{L^\infty([-1,1])}\\
&+\left\|\mathsf{P}_k\left[g'\right]\right\|_{L^\infty([-1,1])}\left\|\mathsf{P}_k\left[p_b\right]-p_b\right\|_{L^\infty([-1,1])}\\
\leq&\,4\epsilon\|g'\|_{L^\infty([-1,1])}\|p_b\|_{L^\infty([-1,1])}.
\end{aligned} \tag{129}$$

Now (124) and (129) imply the first inequality in (122), and the second follows from (119) and (120).

Combining (118) with (122) and (126) shows that

$$\begin{aligned}
&\left|\mathsf{P}_k\left[p_b\right]'(x)+\mathsf{P}_k\left[g'\right](x)\mathsf{P}_k\left[p_b\right](x)-\mathsf{P}_{2k}\left[f\right](x)\right|\\
\leq&\epsilon\left(1+\left(1+(1+4G_1)\,C(W_0)\min\left\{1,\frac{1}{|W|}\right\}\right)\frac{|W|}{G_0}\right)\|f\|_{L^\infty([-1,1])}\\
\leq&\epsilon\left(2+(1+4G_1)\,C(W_0)\min\left\{1,\frac{1}{|W|}\right\}\right)\frac{|W|}{G_0}\|f\|_{L^\infty([-1,1])},
\end{aligned} \tag{130}$$

for all $x\in[-1,1]$, since $G_0\leq|W|$. If we now let

$$\mathbf{p_b}=\begin{pmatrix}p_b\left(x_{1,k}^{\text{cheb}}\right)\\p_b\left(x_{2,k}^{\text{cheb}}\right)\\\vdots\\p_b\left(x_{k,k}^{\text{cheb}}\right)\end{pmatrix},\quad\mathbf{f}=\begin{pmatrix}f\left(x_{1,2k}^{\text{cheb}}\right)\\f\left(x_{2,2k}^{\text{cheb}}\right)\\\vdots\\f\left(x_{2k,2k}^{\text{cheb}}\right)\end{pmatrix} \tag{131}$$

and define the $2k \times 2k$ diagonal matrix $\mathscr{G}_{2k}$ via

$$\mathscr{G}_{2k} = \begin{pmatrix} g'\left(x^{\text{cheb}}_{1,2k}\right) & & & \\ & g'\left(x^{\text{cheb}}_{2,2k}\right) & & \\ & & \ddots & \\ & & & g'\left(x^{\text{cheb}}_{2k,2k}\right) \end{pmatrix}, \tag{132}$$

then (130) implies that

$$\left(\mathscr{I}_{2k,k}\mathscr{D}_k + i\mathscr{G}_{2k}\mathscr{I}_{2k,k}\right)\mathbf{p_b} = \mathbf{f} + \boldsymbol{\delta}\mathbf{f}, \tag{133}$$

with

$$\|\mathbf{p_b}\|_2 \lesssim C(W_0)\frac{|W|}{G_0}\min\left\{1, \frac{1}{|W|}\right\}\|f\|_{L^\infty([-1,1])} \tag{134}$$

and

$$\|\boldsymbol{\delta}\mathbf{f}\|_2 \lesssim \epsilon\left(2 + (1+4G_1)\,C(W_0)\min\left\{1, \frac{1}{|W|}\right\}\right)\frac{|W|}{G_0}\|f\|_{L^\infty([-1,1])}, \tag{135}$$

where the matrices $\mathscr{D}_k$ and $\mathscr{I}_{2k,k}$ are defined in Section 2.2; $\mathscr{D}_k$ is the $k \times k$ spectral differentiation matrix and $\mathscr{I}_{2k,k}$ is is the matrix which interpolates polynomials of degree k from the k-point Chebyshev grid to the $2k$-point Chebyshev grid. Recall from Subsection 2.1 that we use notation $x \lesssim y$ to indicate that there is some constant C not depending on either x or y, such that $x \leq Cy$. We introduce the notation

$$\mathscr{A}_k = \mathscr{I}_{2k,k}\mathscr{D}_k + i\mathscr{G}_{2k}\mathscr{I}_{2k,k} \tag{136}$$

in order to simplify the following discussion. Notice now that

$$\max\{G_1, 1\}\min\left\{1, \frac{1}{|W|}\right\} \geq 1, \tag{137}$$

since $|W| \leq G_1$. From (134), (135), (137), and the fact that

$$\|\mathscr{A}_k\|_2 \lesssim \max\{G_1, 1\}, \tag{138}$$

we see that

$$\|\boldsymbol{\delta}\mathbf{f}\|_2 \lesssim \epsilon\,\|\mathscr{A}_k\|_2\,\|\mathbf{p_b}\|_2\,, \tag{139}$$

regardless of the magnitude of g'. By Corollary 2, when we solve the linear system

$$\mathscr{A}_k\mathbf{p} = \mathbf{f} \tag{140}$$

via a singular value decomposition which has been truncated at precision $\epsilon\,\|\mathscr{A}_k\|_2$, we obtain a solution $\widehat{\mathbf{p}}$ such that

$$\|\widehat{\mathbf{p}}\|_2 \lesssim \|\mathbf{p_b}\|_2 \lesssim C(W_0)\frac{|W|}{G_0}\min\left\{1, \frac{1}{|W|}\right\}\|f\|_{L^\infty([-1,1])} \tag{141}$$

and

$$\begin{aligned}\|\mathscr{A}_k\widehat{\mathbf{p}}-\mathbf{f}\|_2 &\lesssim \epsilon\,\|\mathscr{A}_k\|_2\,\|\mathbf{p_b}\|_2\\ &\lesssim \epsilon\,C(W_0)\frac{|W|}{G_0}\max\{G_1,1\}\min\left\{1,\frac{1}{|W|}\right\}\|f\|_{L^\infty([-1,1])}.\end{aligned}\tag{142}$$

We now let $\widehat{p}$ be the k-term Chebyshev expansion whose values at the nodes of the k-point extremal Chebyshev grid agree with the values of the vector $\widehat{\mathbf{p}}$, and we let $\widehat{\delta f}$ be the $2k$-term Chebyshev expansion whose values at the nodes of the $2k$-point extremal Chebyshev grid equal the entries of the vector $\widehat{\boldsymbol{\delta}\mathbf{f}}$ given by the formula $\widehat{\boldsymbol{\delta}\mathbf{f}}=\mathscr{A}_k\widehat{\mathbf{p}}-\mathbf{f}$. From (141) and (142) and the fact that the Chebyshev polynomials are bounded in $L^\infty([-1,1])$ norm by 1, we have that

$$\|\widehat{p}\|_{L^\infty([-1,1])}\lesssim C(W_0)\frac{|W|}{G_0}\min\left\{1,\frac{1}{|W|}\right\}\|f\|_{L^\infty([-1,1])}\tag{143}$$

and

$$\|\widehat{\delta f}\|_{L^\infty([-1,1])}\lesssim \epsilon\,C(W_0)\frac{|W|}{G_0}\max\{G_1,1\}\min\left\{1,\frac{1}{|W|}\right\}\|f\|_{L^\infty([-1,1])}.\tag{144}$$

To see that $\widehat{p}$ satisfies the Levin equation to high accuracy, we first observe that, by the definiton of $\widehat{\boldsymbol{\delta}\mathbf{f}}$,

$$\widehat{p}'\left(x_{j,2k}^{\text{cheb}}\right)+ig'\left(x_{j,2k}^{\text{cheb}}\right)\widehat{p}\left(x_{j,2k}^{\text{cheb}}\right)=f\left(x_{j,2k}^{\text{cheb}}\right)+\widehat{\delta f}\left(x_{j,2k}^{\text{cheb}}\right)\tag{145}$$

for all $j=1,\ldots,2k$. That is,

$$\mathsf{P}_{2k}\left[\widehat{p}'\right](x)+i\mathsf{P}_{2k}\left[g'\widehat{p}\right](x)=\mathsf{P}_{2k}\left[f\right](x)+\mathsf{P}_{2k}[\widehat{\delta f}](x).\tag{146}$$

Since $\widehat{p}$ and $\widehat{\delta f}$ are polynomials of degrees k and $2k$, respectively, (146) implies

$$\widehat{p}'(x)+i\mathsf{P}_{2k}\left[g'\widehat{p}\right](x)=\mathsf{P}_{2k}\left[f\right](x)+\widehat{\delta f}(x).\tag{147}$$

Using (125), (143) and the fact that $\mathsf{P}_k\left[g'\right](x)\widehat{p}(x)$ is a polynomial of degree $2k$, we see that

$$\begin{aligned}|\mathsf{P}_{2k}\left[g'\widehat{p}\right](x)-g'(x)\widehat{p}(x)| &\le |\mathsf{P}_{2k}\left[g'\widehat{p}\right](x)-\mathsf{P}_k\left[g'\right](x)\widehat{p}(x)|\\ &\quad+|\mathsf{P}_k\left[g'\right](x)\widehat{p}(x)-g'(x)\widehat{p}(x)|\\ &\le \Lambda_{2k}\,\|\widehat{p}\|_{L^\infty([-1,1])}\,|g'(x)-\mathsf{P}_k\left[g'\right](x)|\\ &\quad+\|\widehat{p}\|_{L^\infty([-1,1])}\,|\mathsf{P}_k\left[g'\right](x)-g'(x)|\\ &\le \epsilon\,(1+\Lambda_{2k})\,\|g'\|_{L^\infty([-1,1])}\,\|\widehat{p}\|_{L^\infty([-1,1])}\\ &\lesssim \epsilon\,C(W_0)|W|\frac{G_1}{G_0}\min\left\{1,\frac{1}{|W|}\right\}\|f\|_{L^\infty([-1,1])},\end{aligned}\tag{148}$$

for all $x\in[-1,1]$, where Λ_{2k} denotes the Lebesgue constant of the $2k$-point extremal Chebyshev grid. From (126), (144), (147) and (148), we finally arrive

at the inequality

$$\begin{aligned}
&|\widehat{p}'(x) + ig'(x)\widehat{p}(x) - f(x)| \\
\leq &|\widehat{\delta f}(x)| + |P_{2k}[f](x) - f(x)| + |P_{2k}\left[g'\widehat{p}\right](x) - g'(x)\widehat{p}(x)| \\
\lesssim &\epsilon \left(1 + (G_1 + \max\{G_1, 1\})\, C(W_0) \frac{|W|}{G_0} \min\left\{1, \frac{1}{|W|}\right\}\right) \|f\|_{L^\infty([-1,1])} \\
\lesssim &\epsilon\, C(W_0) \frac{|W|}{G_0} \max\{G_1, 1\} \min\left\{1, \frac{1}{|W|}\right\} \|f\|_{L^\infty([-1,1])},
\end{aligned} \tag{149}$$

which holds for all $x \in [-1, 1]$.

To complete our analysis for the case in which $G_0 > 0$, we let

$$I = \int_{-1}^{1} f(t) \exp(ig(t))\, dt \tag{150}$$

be the true value of the oscillatory integral we hope to compute via the Levin method, and take $\widehat{I}$ to be the estimate

$$\widehat{I} = \widehat{p}(1) \exp(ig(1)) - \widehat{p}(-1) \exp(ig(-1)) \tag{151}$$

of I computed using the obtained solution of the Levin equation. Now

$$\begin{aligned}
\widehat{I} - I &= \int_{-1}^{1} \frac{d}{dt} \left(\widehat{p}(t) \exp(ig(t))\right) dt - \int_{-1}^{1} f(t) \exp(ig(t))\, dt \\
&= \int_{-1}^{1} \left(\widehat{p}'(t) + ig'(t)\widehat{p}(t) - f(t)\right) \exp(ig(t))\, dt,
\end{aligned} \tag{152}$$

and it follows from this and (149) that

$$|\widehat{I} - I| \lesssim \epsilon\, C(W_0) \frac{|W|}{G_0} \max\{G_1, 1\} \min\left\{1, \frac{1}{|W|}\right\} \|f\|_{L^\infty([-1,1])}. \tag{153}$$

The quantity

$$|W| \min\left\{1, \frac{1}{|W|}\right\} \tag{154}$$

is clearly bounded independently of the magnitude of g'. Moreover, G_1/G_0 is small when g' does not vary in magnitude too much over the interval (a reasonable assumption when analyzing an adaptive scheme). So (153) shows that the absolute error in the computed integral is bounded independently of the magnitude of g', assuming g' does not vary too much over the interval.

4.2 The case when $G_1 < 1/4$

We now consider the case in which $G_1 < 1/4$. By invoking Theorem 5, we can find a bandlimited function p_b such that

$$|p_b'(x) + ig'(x)p_b(x) - f(x)| \leq 2\epsilon \left(1 + \frac{G_1}{1 - 2G_1}\right) \|f\|_{L^\infty([-1,1])} \tag{155}$$

for all $x \in [-1,1]$, where

$$\|p_b\|_{L^\infty([-1,1])} \leq \frac{2}{1-2G_1}\|f\|_{L^\infty([-1,1])} \tag{156}$$

and

$$\|p_b'\|_{L^\infty([-1,1])} \leq 4\left(1+\frac{G_1}{1-2G_1}\right)\|f\|_{L^\infty([-1,1])}. \tag{157}$$

Since our assumption on the maximum size of G_1 implies a bound on the maximum bandlimit of p_b, the Chebyshev coefficients of p_b are bounded by a rapidly decaying function which is independent of G_1. Moreover, we can once again choose k independently of G_1 such that (123) through (129) hold. Then, proceeding as we did before, we see that

$$\begin{aligned} &\left\|\mathsf{P}_k\left[p_b\right]' + i\mathsf{P}_k\left[g'\right]\mathsf{P}_k\left[p_b\right] - \left(p_b' + ig'p_b\right)\right\|_{L^\infty([-1,1])} \\ \lesssim_\epsilon &\left(1+\frac{G_1}{1-2G_1}\right)\|f\|_{L^\infty([-1,1])} \end{aligned} \tag{158}$$

for all $x \in [-1,1]$. If we define $\mathbf{p_b}$, $\mathbf{f}$, $\boldsymbol{\delta}\mathbf{f}$ and $\mathscr{A}_k$ as before, then we see that

$$\|\boldsymbol{\delta}\mathbf{f}\|_2 \lesssim \epsilon\left(1+\frac{G_1}{1-2G_1}\right)\|f\|_{L^\infty([-1,1])} \tag{159}$$

while

$$\|\mathscr{A}_k\|_2\,\|\mathbf{p_b}\|_2 \lesssim \frac{1}{1-2G_1}\max\{G_1,1\}\|f\|_{L^\infty([-1,1])}, \tag{160}$$

so there is no difficulty in applying Corollary 2 to see that solving (140) via a truncated singular value decomposition yields a vector $\widehat{\mathbf{p}}$ such that

$$\|\widehat{\mathbf{p}}\|_2 \lesssim \frac{1}{1-2G_1}\|f\|_{L^\infty([-1,1])} \tag{161}$$

and

$$\begin{aligned} \|\mathscr{A}_k\widehat{\mathbf{p}} - \mathbf{f}\|_2 &\lesssim \epsilon\,\|\mathscr{A}_k\|_2\,\|\mathbf{p_b}\|_2 \\ &\lesssim \epsilon\max\{G_1,1\}\frac{1}{1-2G_1}\|f\|_{L^\infty([-1,1])}. \end{aligned} \tag{162}$$

Defining $\widehat{p}$ and $\widehat{\delta f}$ as before, we obtain the bound

$$\begin{aligned} &|\widehat{p}'(x) + ig'(x)\widehat{p}(x) - f(x)| \\ \lesssim &\epsilon\left(1+\max\{G_1,1\}\frac{1}{1-2G_1}+\frac{G_1}{1-2G_1}\right)\|f\|_{L^\infty([-1,1])} \\ \lesssim &\epsilon\left(\frac{1}{1-2G_1}\right)\|f\|_{L^\infty([-1,1])}, \end{aligned} \tag{163}$$

which holds for all $x \in [-1, 1]$. It follows from this that the absolute error in the computed value $\widehat{I}$ approximating the integral I defined by (151) satisfies

$$|\widehat{I} - I| \lesssim \epsilon \left(\frac{1}{1 - 2G_1} \right) \|f\|_{L^\infty([-1,1])}. \tag{164}$$

This bound grows as G_1 approaches $1/2$, but since we are considering an interval on which $G_1 < 1/4$, the constant in (164) is small.

5 The Adaptive Levin Method

In this section, we describe the adaptive Levin method for the numerical calculation of the integral

$$\int_a^b f(x) \exp(ig(x))\, dx. \tag{165}$$

Trivial modifications allow for the evaluation of

$$\int_a^b f(x) \cos(g(x))\, dx \quad \text{or} \quad \int_a^b f(x) \sin(g(x))\, dx \tag{166}$$

instead.

Although the rigorous analysis presented in the preceding section concerns a spectral collocation method in which the solution of the equation is represented via k discretization nodes while the equation is required to hold at $2k$ discretization nodes, the algorithm we describe here only enforces the Levin equation at k discretization nodes. The properties of the algorithm are barely affected by this change, and we now explain why this is the case.

When the Levin method is used adaptively, subintervals are typically divided until f and g' can be represented by polynomials of degree much lower than k. This is simply because adaptive procedures are typically suboptimal and usually lead to the over-discretization of their inputs. If g' is large and such over-discretization has taken place, the obtained solution $\widehat{p}$ will also be a polynomial of degree somewhat lower than k. This is because the discretized Levin equation does not have a nontrivial nullspace when g' is large, and so $\widehat{p}$ will closely agree with the nonoscillatory solution p_b, which can be represented by a polynomial of low degree. So in the case when g' is large, the product $g'\widehat{p}$ can often be represented accurately via a polynomial of degree k.

On the other hand, when g' is small enough, the discretized nullspace is nontrivial, but its elements can be represented by polynomials of low degree. Consequently, in this case, the product $g'\widehat{p}$ can also often be represented by a polynomial of degree k.

It is only when g' is of moderate size, but not "large" or "small," that we expect $g'\widehat{p}$ to be of degree larger than k. Accordingly, when an adaptive Levin method which only enforces the Levin equation at k discretization points is used, only those intervals on which g' falls into a relatively narrow range of

moderate values will require additional subdivision. Thus, we do not expect many additional subdivisions to occur.

Before detailing the algorithm proper, we describe a subroutine which estimates the value of

$$\int_{a_0}^{b_0} f(x) \exp(ig(x))\, dx, \tag{167}$$

where $[a_0, b_0]$ is a subinterval of $[a, b]$. It takes as input the interval $[a_0, b_0]$, an integer k which controls the number of Chebyshev nodes used to discretize the Levin equation, an absolute tolerance parameter $\epsilon_0 > 0$, and an external subroutine for evaluating the functions f and g. The subroutine proceeds as follows:

1. Use the external subroutine supplied by the user to evaluate the functions f and g at the extremal Chebyshev nodes translated from $[-1, 1]$ to the interval $[a_0, b_0]$, which we also denote by $x_{1,k}^{\text{cheb}},\ x_{2,k}^{\text{cheb}},\ \ldots,\ x_{k,k}^{\text{cheb}}$.
2. Calculate approximate values

$$\widetilde{g'\left(x_{1,k}^{\text{cheb}}\right)},\ \ldots,\ \widetilde{g'\left(x_{k,k}^{\text{cheb}}\right)} \tag{168}$$

of the derivatives of the function g at the extremal Chebyshev nodes by applying the spectral differentiation matrix $\mathscr{D}_k$ to the vector of values of g; that is, via the formula

$$\begin{pmatrix} \widetilde{g'\left(x_{1,k}^{\text{cheb}}\right)} \\ \widetilde{g'\left(x_{2,k}^{\text{cheb}}\right)} \\ \vdots \\ \widetilde{g'\left(x_{k,k}^{\text{cheb}}\right)} \end{pmatrix} = \mathscr{D}_k \begin{pmatrix} g\left(x_{1,k}^{\text{cheb}}\right) \\ g\left(x_{2,k}^{\text{cheb}}\right) \\ \vdots \\ g\left(x_{k,k}^{\text{cheb}}\right) \end{pmatrix}. \tag{169}$$

3. Form the matrix

$$\mathscr{A} = \mathscr{D}_k + i \begin{pmatrix} \widetilde{g'\left(x_{1,k}^{\text{cheb}}\right)} & & & \\ & \widetilde{g'\left(x_{2,k}^{\text{cheb}}\right)} & & \\ & & \ddots & \\ & & & \widetilde{g'\left(x_{k,k}^{\text{cheb}}\right)} \end{pmatrix}. \tag{170}$$

4. Construct a singular value decomposition

$$\mathscr{A} = \begin{pmatrix} \mathbf{u_1} & \mathbf{u_2} & \cdots & \mathbf{u_k} \end{pmatrix} \begin{pmatrix} \sigma_1 & & & \\ & \sigma_2 & & \\ & & \ddots & \\ & & & \sigma_k \end{pmatrix} \begin{pmatrix} \mathbf{v_1} & \mathbf{v_2} & \cdots & \mathbf{v_k} \end{pmatrix}^* \tag{171}$$

of the matrix $\mathscr{A}$.

5. Find the greatest integer $1 \leq l \leq k$ such that $\sigma_l \geq \|\mathscr{A}\|_2 \epsilon_0$. If no such integer exists, return the estimate 0 for (167).
6. Let

$$\begin{pmatrix} \widetilde{p\left(x_{1,k}^{\mathrm{cheb}}\right)} \\ \widetilde{p\left(x_{2,k}^{\mathrm{cheb}}\right)} \\ \vdots \\ \widetilde{p\left(x_{k,k}^{\mathrm{cheb}}\right)} \end{pmatrix} = \begin{pmatrix} \mathbf{v_1} & \cdots & \mathbf{v_l} \end{pmatrix} \begin{pmatrix} \frac{1}{\sigma_1} & & & \\ & \frac{1}{\sigma_2} & & \\ & & \ddots & \\ & & & \frac{1}{\sigma_l} \end{pmatrix} \begin{pmatrix} \mathbf{u_1} & \cdots & \mathbf{u_l} \end{pmatrix}^* \begin{pmatrix} f\left(x_{1,k}^{\mathrm{cheb}}\right) \\ f\left(x_{2,k}^{\mathrm{cheb}}\right) \\ \vdots \\ f\left(x_{k,k}^{\mathrm{cheb}}\right) \end{pmatrix}.$$

The entries of this vector approximate the values of a function p such that

$$\frac{d}{dx}\left(p(x)\exp(ig(x))\right) = f(x)\exp(ig(x)) \tag{172}$$

at the extremal Chebyshev nodes on $[a_0, b_0]$.

7. Return the estimate

$$\widetilde{p\left(x_{k,k}^{\mathrm{cheb}}\right)} \exp\left(ig\left(x_{k,k}^{\mathrm{cheb}}\right)\right) - \widetilde{p\left(x_{1,k}^{\mathrm{cheb}}\right)} \exp\left(ig\left(x_{1,k}^{\mathrm{cheb}}\right)\right) \tag{173}$$

for the value of (167).

The algorithm proper takes as input an absolute tolerance parameter $\epsilon > \epsilon_0 > 0$, the endpoints $a < b$ of the integration domain, an integer k specifying the number of Chebyshev nodes used to discretize the Levin equation on each subinterval considered, and an external subroutine which returns the values of the functions f and g at a specified collection of points. It maintains an estimated value *val* for (165) and a list of intervals. Initially, the list of intervals contains only $[a, b]$ and the value of the estimate is set to 0. As long as the list of intervals is nonempty the following steps are repeated:

1. Remove an entry $[a_0, b_0]$ from the list of intervals.
2. Calculate an estimate val_0 of

$$\int_{a_0}^{b_0} f(x)\exp(ig(x))\,dx \tag{174}$$

using the subprocedure described above.

3. Calculate estimates val_{L} and val_{R} of
$$\int_{a_0}^{c_0} f(x)\exp(ig(x))\,dx \quad \text{and} \quad \int_{c_0}^{b_0} f(x)\exp(ig(x))\,dx, \tag{175}$$
where $c_0 = (a_0 + b_0)/2$, using the subprocedure described above.
4. If $|val_0 - val_{\text{L}} - val_{\text{R}}| < \epsilon$, then update the estimate val by letting $val = val + val_0$. Otherwise, add the intervals $[a_0, c_0]$ and $[c_0, b_0]$ to the list of intervals.

In the end, the procedure returns the estimate val for (165). Because the condition number of the oscillatory integral (165) increases with the magnitude of g', some loss of accuracy is expected when calculating its value numerically. In the case of the adaptive Levin method, the principal loss of accuracy occurs when exponentials of large magnitude are evaluated in (173). Of course, the magnitudes of many integrals of the form (165) decrease with the magnitude g', with the consequence that the absolute error in the calculated value of (165) often remains constant or even decays as the magnitude of g' increases.

Remark 2. *The truncated singular value decomposition is quite expensive. In our implementation of the adaptive Levin method, we used a rank-revealing QR decomposition in lieu of the truncated singular value decomposition to solve the linear system which results from discretizing the ordinary differential equation. This was found to be about 5 times faster and leads to no apparent loss in accuracy.*

Remark 3. *While it may be more accurate to let* $val = val + val_{L} + val_{R}$ *rather than* $val = val + val_0$ *in Step 4 of the algorithm, we choose the latter for the sake of simplicity.*

6 Phase Functions for Ordinary Differential Equations

Many integrals of interest involve special functions which satisfy second order linear ordinary differential equations. To give one simple example, the Hankel transform $H_\nu[f](k)$ of the function $f(x)$ is defined via the formula
$$H_\nu[f](k) = \int_0^\infty J_\nu(kx)\sqrt{kx}f(x)\,dx, \tag{176}$$
where $J_\nu(z)$ denotes the Bessel function of the first kind of order ν. The function $J_\nu(z)$ is, of course, a solution of Bessel's differential equation
$$z^2y''(z) + zy'(z) + (z^2 - \nu^2)y(z) = 0. \tag{177}$$

We say that α is a phase function for

$$y''(t) + p(t)y'(t) + q(t)y(t) = 0, \qquad a < t < b, \tag{178}$$

provided α' is positive on (a, b) and the pair

$$u(t) = \sqrt{\frac{\omega(t)}{\alpha'(t)}}\cos(\alpha(t)) \quad \text{and} \quad v(t) = \sqrt{\frac{\omega(t)}{\alpha'(t)}}\sin(\alpha(t)), \tag{179}$$

where $\omega(t) = \exp\left(-\int p(t)\,dt\right)$, constitute a basis in the space of solutions of (178). We note that it is a consequence of Abel's identity that the Wronskian of any pair of independent solutions of (178) is $\omega(t)$. It has long been known that the solutions of second order linear ordinary differential equations with slowly varying coefficients can be represented by slowly varying phase functions, even in cases in which the solutions themselves are highly oscillatory or behave like linear combinations of rapidly increasing and decreasing exponentials. This observation is the basis of the WKB method (see, for instance, Chapter 7 of [9]) and many other related asymptotic techniques (for example, [24], [13], [11] and [12]).

It follows that many integrals involving classical functions — such as (176) — can be put into one of the forms

$$\int f(x)\exp(ig(x))\,dx, \quad \int f(x)\cos(g(x))\,dx \quad \text{or} \quad \int f(x)\sin(g(x))\,dx \tag{180}$$

with f and g slowly varying. Integrals of this type are, of course, highly amenable to calculation via the adaptive Levin method, provided the relevant phase function $g(x)$ can be evaluated efficiently.

In [16], a numerical algorithm for constructing slowly varying phase functions for second order linear ordinary differential equations whose solutions are oscillatory is introduced. Under mild conditions on the coefficients, it runs in time independent of the frequency of oscillations of the solutions and achieves accuracy on par with the condition number of the problem. A companion paper [14] provides a bound on the complexity of the phase function calculated by the algorithm of [16].

In [17], the algorithm of [16] is extended to the case of second order linear ordinary differential equations with turning points — that is, it applies to equations whose solutions oscillate in some regions and behave like linear combinations of increasing and decreasing exponentials in others. In many cases of interest, it runs in time independent of the magnitude of the coefficients and obtains accuracy in line with the condition number of the equation. Phase functions which represent many classical special functions — including the Bessel functions, associated Legendre functions, spheroidal wave functions, Hermite polynomials, and the Jacobi polynomials — can be efficiently calculated using the algorithm of [17], which the numerical experiments discussed in Subsections 7.4 and 7.6 make use of.

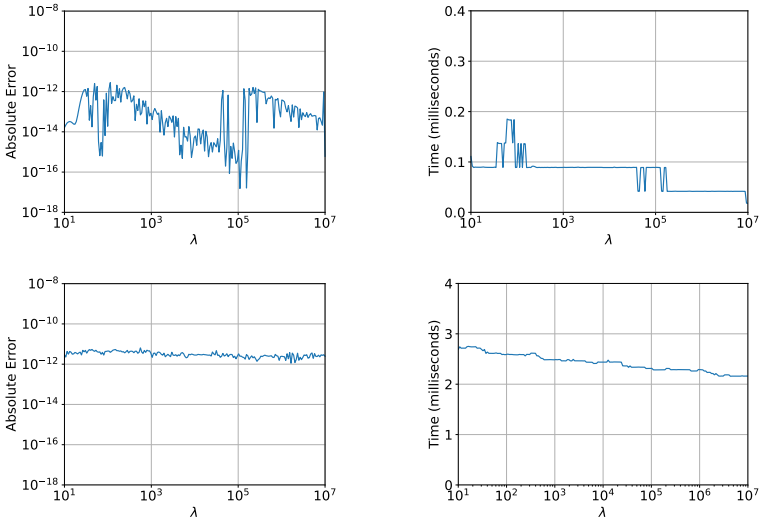

Fig. 1: The results of the first two experiments of Section 7.1. The first row of plots pertains to the integral I_1 and the second to I_2. Each plot on the left gives the error in the value of the integral computed via the adaptive Levin method as a function of λ, while each plot on the right gives the running time in milliseconds as a function of λ.

7 Numerical experiments

In this section, we present the results of numerical experiments which were conducted to illustrate the properties of the algorithm of this article. The code for these experiments was written in Fortran and compiled with version 12.10 of the GNU Fortran compiler. They were performed on a desktop computer equipped with an AMD Ryzen 3900X processor and 32GB of memory. No attempt was made to parallelize our code. We used a 12-point Chebyshev spectral method in our implementation of the adaptive Levin scheme (i.e., the parameter k was taken to be 12). As discussed in Section 5, the condition number of evaluation of most integrals of the form

$$\int_a^b f(x)\exp(ig(x))\,dx \tag{181}$$

increases with the magnitude of g'. This is often offset by a commensurate decrease in the magnitude of the integral with the consequence that, in most cases, it is reasonable to expect absolute errors in the calculated values of (181) to be largely independent of the magnitude of g'. Unless mentioned otherwise, we set the absolute tolerance parameter to be $\epsilon = 10^{-12}$, and set ϵ_0 to be equal to machine precision.

In order to estimate the error in the results produced by the adaptive Levin method, we compared the results of the adaptive Levin method with the results

produced by adaptive Gaussian quadrature for evaluating integrals of the from

$$\int_a^b f(x)\,dx, \quad -\infty < a < b < \infty. \tag{182}$$

We use this method to estimate the error in every case, except when explicit formulas for the integrals are available. Our implementation of the adaptive Gaussian quadrature algorithm is written is Fortran and is quite standard. It maintains a list of intervals, which is initialized with the single interval $[a, b]$, and a running tally of the value of the integral, which is initialized to zero. As long as the list of intervals is nonempty, the algorithm removes one interval $[a_0, b_0]$ from the list, compares the value of

$$\int_{a_0}^{b_0} f(x)\,dx \tag{183}$$

as computed by a 30-point Gauss-Legendre quadrature rule to the value of the sum

$$\int_{a_0}^{(a_0+b_0)/2} f(x)\,dx + \int_{(a_0+b_0)/2}^{b_0} f(x)\,dx, \tag{184}$$

where each integral is separately estimated with a 30-point Gauss-Legendre rule. If the difference is larger than ϵ, where ϵ is a tolerance parameter supplied by the user, then the intervals $[a_0, (a_0 + b_0)/2]$ and $[(a_0 + b_0)/2, b_0]$ are placed in the list of intervals. Otherwise, the value of (183) is added to the running tally of the value of the integral (182). In all of the experiments described here, the tolerance parameter for the adaptive Gaussian quadrature code was taken to be $\epsilon = 10^{-15}$. We found it necessary to set the tolerance parameter for adaptive Gaussian quadrature to be somewhat smaller than that for the adaptive Levin method in order to obtain accurate results from the former. We used a 30-point Gauss-Legendre rule because we found it to be more efficient than rules of other orders in most cases.

In Subsection 7.1, we consider oscillatory integrals for which analytical formulas are available, and present plots of runtimes and errors of the adaptive Levin method over a wide range of frequencies. We then present, in Subsection 7.2, experiments for some oscillatory integrals for which such analytical formulas are not readily available. We assess the accuracy of the adaptive Levin method by comparing against results computed by adaptive Gaussian quadrature, and provide a detailed comparison of performance between the two methods, over a wide range of frequencies. In Subsection 7.3, we demonstrate the performance of the adaptive Levin method for an integral with a stationary point of order m, and provide a theoretical analysis explaining the expected behavior.

The experiments of Subsections 7.4–7.7 concern integrals involving special functions, namely, the Bessel functions, the associated Legendre functions and the Hermite polynomials. In order to apply the adaptive Levin method to integrals involving these functions, we constructed phase function representations

of them via the method of [17]. That algorithm applies to second order linear ordinary differential equations of the form

$$y''(x) + q(x)y(x) = 0, \quad a < x < b, \tag{185}$$

where the coefficient q is real-valued and slowly varying. We note that essentially any second order differential equation, including the differential equation defining the associated Legendre functions and Bessel's differential equation, can be put into the form (185) via a simple transformation. The method of [17] constructs a piecewise Chebyshev expansion representing a slowly-varying phase function ψ such that

$$\frac{\exp\left(i\psi(x)\right)}{\sqrt{\psi'(x)}} \quad \text{and} \quad \frac{\exp\left(-i\psi(x)\right)}{\sqrt{\psi'(x)}} \tag{186}$$

constitute a basis in the space of solutions of (185). The derivative of the phase function is uniquely determined, but the phase function itself is only defined up to a constant. We typically use this degree of freedom to ensure that either

$$\frac{\sin\left(\psi(x)\right)}{\sqrt{\psi'(x)}} \quad \text{or} \quad \frac{\cos\left(\psi(x)\right)}{\sqrt{\psi'(x)}} \tag{187}$$

represent the special function we wish to integrate.

In Subsection 7.4, in which we evaluate integrals involving Bessel functions, we report separately the times required for the construction of the phase function and the evaluation of the integral by the adaptive Levin method. We include a direct comparison with adaptive Gaussian integration in Subsection 7.5, in which we also evaluate integrals involving Bessel functions. We use the adaptive Levin method to evaluate the modal Green's functions in Subsection 7.8, which are special functions represented by an integral in which the integrand has two oscillatory components. Lastly, we apply the method to an integral with many stationary points in Subsection 7.9.

7.1 Certain integrals involving elementary functions for which explicit formulas are available

In the experiments described in this subsection, we considered the integrals

$$I_1(\lambda) = \int_{-1}^{1} \cos\left(\lambda \arctan(x)\right) \frac{1}{1+x^2}\, dx = \frac{2}{\lambda} \sin\left(\frac{\pi\lambda}{4}\right),$$

$$I_2(\lambda) = \int_{0}^{\infty} \frac{\exp\left(i\lambda x^2\right)}{\sqrt{x}}\, dx = \exp\left(\frac{\pi i}{8}\right) \frac{2\Gamma\left(\frac{5}{4}\right)}{\lambda^{\frac{1}{4}}},$$

$$I_3(\lambda) = \int_{0}^{1} \exp\left(\frac{i\lambda}{\sqrt{x}}\right) \frac{1}{x}\, dx = 2\Gamma(0, -i\lambda) \quad \text{and}$$

$$I_4(\lambda) = \int_{0}^{10} \exp(i\lambda \exp(x)) \exp(x)\, dx = \frac{i}{\lambda} \left(\exp(i\lambda) - \exp\left(i \exp\left(10\right) \lambda\right)\right).$$

All of the above formulas can be found in [25].

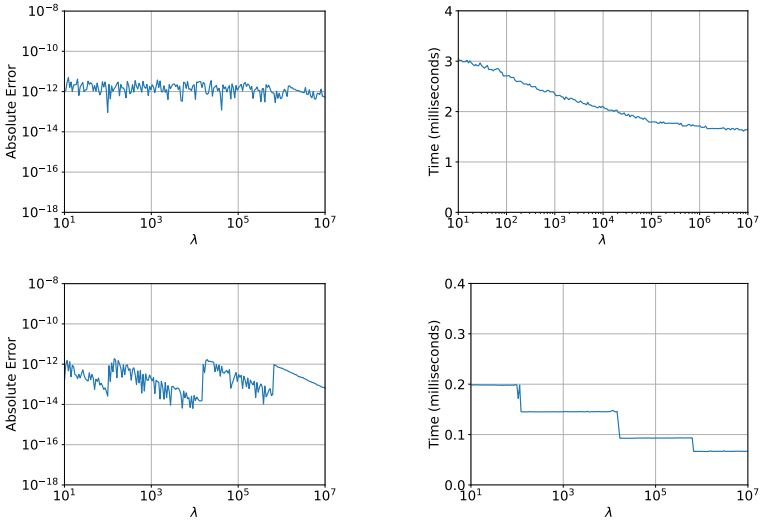

Fig. 2: The results of the last two experiments of Section 7.1. The first row of plots pertains to the integral I_3 and the second to I_4. Each plot on the left gives the error in the value of the integral computed via the adaptive Levin method as a function of λ, while each plot on the right gives the running time in milliseconds as a function of λ.

We proceeded by first sampling $l = 200$ equispaced points $x_1, \ldots, x_l$ in the interval $[1, 7]$. Then, we used the adaptive Levin method to evaluate the integrals appearing above for each $\lambda = 10^{x_1}, 10^{x_2}, \ldots, 10^{x_l}$. Figures 1 and 2 give the time required to evaluate these integrals and the absolute errors in the obtained values.

7.2 Certain other integrals involving elementary functions

In the experiments of this subsection, we evaluated the integrals

$$\begin{aligned} I_5(\lambda) &= \int_0^1 \exp\left(i\lambda x^2\right) \exp\left(-x\right) x \, dx, \\ I_6(\lambda) &= \int_{-1}^1 \exp\left(i\lambda x^2\right) \left(1 + x^2\right) \, dx, \\ I_7(\lambda) &= \int_{-4}^4 \exp\left(i\lambda x^2\right) \, dx \quad \text{and} \\ I_8(\lambda) &= \int_{-1}^1 \exp\left(i\lambda x^4\right) \frac{1}{0.01 + x^4} \, dx. \end{aligned} \tag{188}$$

We considered various ranges of values of λ. We randomly sampled 200 values of λ in each range and then, for each such value of λ, we calculated I_5, I_6, I_7

and I_8 using both the adaptive Levin algorithm and our adaptive Gaussian quadrature code. The time taken by each method was measured, and the absolute differences between the values of the integrals calculated with each method was recorded. Table 1 gives the results. Each row gives the results for one integral and range of values of λ.

Integral	Range of λ	Avg Time Adap Levin	Avg Time Adap Gauss	Ratio	Max Observed Difference
I_5	$10^0 - 10^1$	4.83×10^{-05}	2.23×10^{-06}	0.05	9.94×10^{-13}
	$10^1 - 10^2$	9.16×10^{-05}	5.93×10^{-06}	0.06	1.32×10^{-12}
	$10^2 - 10^3$	1.23×10^{-04}	4.71×10^{-05}	0.38	1.01×10^{-12}
	$10^3 - 10^4$	1.58×10^{-04}	4.15×10^{-04}	2.64	7.53×10^{-13}
	$10^4 - 10^5$	2.02×10^{-04}	4.26×10^{-03}	21.12	9.99×10^{-13}
	$10^5 - 10^6$	2.29×10^{-04}	3.99×10^{-02}	173.87	1.00×10^{-12}
	$10^6 - 10^7$	2.51×10^{-04}	3.71×10^{-01}	1476.94	4.00×10^{-13}
I_6	$10^0 - 10^1$	1.38×10^{-04}	2.29×10^{-06}	0.02	1.94×10^{-12}
	$10^1 - 10^2$	2.88×10^{-04}	1.38×10^{-05}	0.05	1.97×10^{-12}
	$10^2 - 10^3$	4.17×10^{-04}	1.07×10^{-04}	0.26	3.58×10^{-12}
	$10^3 - 10^4$	4.74×10^{-04}	9.00×10^{-04}	1.90	3.32×10^{-12}
	$10^4 - 10^5$	5.25×10^{-04}	8.84×10^{-03}	16.85	2.20×10^{-12}
	$10^5 - 10^6$	5.77×10^{-04}	8.05×10^{-02}	139.52	3.53×10^{-12}
	$10^6 - 10^7$	6.44×10^{-04}	8.01×10^{-01}	1243.52	2.57×10^{-12}
I_7	$10^0 - 10^1$	3.61×10^{-04}	3.03×10^{-05}	0.08	2.57×10^{-12}
	$10^1 - 10^2$	4.84×10^{-04}	2.44×10^{-04}	0.51	2.97×10^{-12}
	$10^2 - 10^3$	5.32×10^{-04}	2.31×10^{-03}	4.34	3.67×10^{-12}
	$10^3 - 10^4$	5.86×10^{-04}	2.24×10^{-02}	38.15	3.41×10^{-12}
	$10^4 - 10^5$	6.35×10^{-04}	2.21×10^{-01}	347.36	2.52×10^{-12}
	$10^5 - 10^6$	6.93×10^{-04}	2.31×10^{-00}	3337.39	3.29×10^{-12}
	$10^6 - 10^7$	7.61×10^{-04}	2.66×10^{-01}	34967.12	5.68×10^{-12}
I_8	$10^0 - 10^1$	8.66×10^{-04}	4.26×10^{-05}	0.05	3.48×10^{-12}
	$10^1 - 10^2$	7.32×10^{-04}	1.70×10^{-04}	0.23	6.57×10^{-12}
	$10^2 - 10^3$	7.58×10^{-04}	1.43×10^{-03}	1.88	4.17×10^{-12}
	$10^3 - 10^4$	7.49×10^{-04}	1.36×10^{-02}	18.09	7.30×10^{-12}
	$10^4 - 10^5$	7.41×10^{-04}	1.31×10^{-01}	177.18	6.40×10^{-12}
	$10^5 - 10^6$	7.57×10^{-04}	1.19×10^{-00}	1570.01	3.62×10^{-12}
	$10^6 - 10^7$	8.23×10^{-04}	1.37×10^{-01}	16697.05	3.76×10^{-12}

Table 1: The results of the experiments of Section 7.2 in which the performance of the adaptive Levin method was compared with the performance of an adaptive Gaussian quadrature scheme. Each row corresponds to one of the integrals $I_5(\lambda)$, $I_6(\lambda)$, $I_7(\lambda)$ or $I_8(\lambda)$ and to one range of values of λ. The average time taken by the adaptive Levin method and by an adaptive Gaussian quadrature scheme, the ratio of the average time taken by the adaptive Gaussian quadrature algorithm to the average time taken by the adaptive Levin method, and the maximum observed difference in the values of the integrals computed using each method are reported.

7.3 Behavior in the presence of a stationary point

In the experiments of this subsection, we considered the integral

$$I_9(\lambda, m) = \int_{-1}^{1} \exp\left(i\lambda x^m\right) \frac{\cos(x)}{1+x^2}\, dx \tag{189}$$

in order to understand the behavior of the adaptive Levin method in the presence of a stationary point.

In the first experiment, we sampled $l = 200$ equispaced points $x_1, \ldots, x_l$ in the interval $[1, 7]$ and, for each $\lambda = 10^{x_1}, 10^{x_2}, \ldots, 10^{x_l}$ and $m = 2, 3, 4, 5$, we evaluated $I_9(\lambda, m)$ twice using the adaptive Levin method. The first time the scheme was executed, the tolerance parameter taken to be $\epsilon = 10^{-12}$. The second time, we set $\epsilon = 10^{-7}$. The results are shown in the first two rows of Figure 3. The first column gives the results for $\epsilon = 10^{-7}$ and the second for $\epsilon = 10^{-12}$. The plots in the first row show the number of subintervals in the adaptively determined subdivision of $[-1, 1]$ used to compute the integral as a function of λ for $m = 2, 3, 4, 5$, while those in the second give the absolute error in the computed value of the integral as a function of λ for $m = 2, 3, 4, 5$.

In a second experiment, for each $m = 2, 3, 4, \ldots, 40$ and $\lambda = 10^2, 10^3, 10^4, 10^5$ we evaluated $I_9(\lambda, m)$ twice using the adaptive Levin method. In the first run, the tolerance parameter was taken to be $\epsilon = 10^{-12}$ and, in the second, it was $\epsilon = 10^{-7}$. The results appear in the third row of Figure 3. Each plot there gives the number of subintervals in the adaptive subdivision of $[-1, 1]$ formed by our algorithm as a function of m for each of the values of λ considered. The plot on the left corresponds to $\epsilon = 10^{-7}$ and the plot on the right to $\epsilon = 10^{-12}$.

We see that, when $\epsilon = 10^{-12}$, the number of subintervals in the adaptive subdivision of $[-1, 1]$ formed by the adaptive Levin method varies only slightly with λ and is largely independent of m. However, when $\epsilon = 10^{-7}$, the number of subintervals grows roughly logarithmically with λ and decreases as m increases, for small values of m. It is essentially independent of m for moderate to large values of m.

This behavior can be understood in light of the analysis presented in Section 3. Theorem 5 implies that the Levin method will yield an accurate result on subintervals of the form $[-\delta, \delta]$ provided g' is sufficiently small there. Theorem 4 indicates that the Levin method will yield an accurate result on any subinterval of $[-1, 1]$ which is bounded away from 0 provided the ratio of the maximum to minimum absolute value of g' is small and

$$h(z) = f\left(u^{-1}(z)\right) \frac{du^{-1}}{dz}(z) = \frac{f\left(\operatorname{sign}(z)\, |z|^{\frac{1}{m}}\right)}{m|z|^{1-\frac{1}{m}}} \tag{190}$$

can be represented via a well-behaved function with a small bandlimit there. That h can be represented by a function with small bandlimit is more-or-less

equivalent to the requirement that h be represented via a Chebyshev expansion of small fixed order. We expect the adaptive Levin method to subdivide $[-1, 1]$ until one or both of Theorems 4 and 5 apply to each of the resulting subintervals.

Since $g'(x) = \lambda m x^{m-1}$, in order for $|g'(x)|$ to be bounded by a constant C on $[-\delta, \delta]$, we must have

$$\delta < \left(\frac{C}{m\lambda}\right)^{\frac{1}{m-1}}. \tag{191}$$

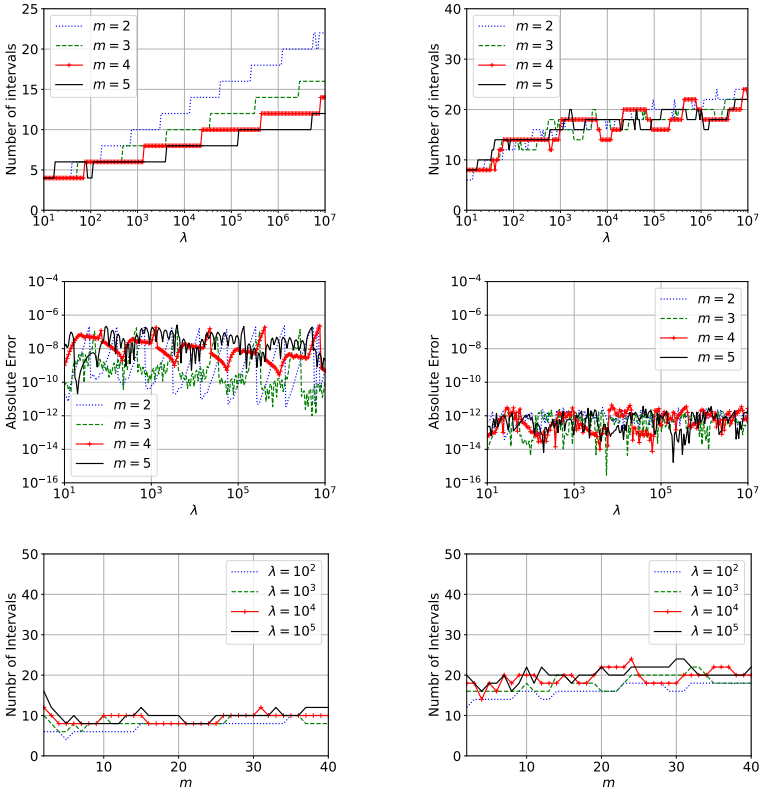

Fig. 3: The results of the experiments of Section 7.3. The plots in the first row give the number of subintervals in the adaptive discretization of $[-1, 1]$ formed in the course of evaluating $I_9(\lambda, m)$ as a function of λ for $m = 2, 3, 4, 5$; those in the second give the absolute error in the calculated error in the value of $I_9(\lambda, m)$ as a function of λ for $m = 2, 3, 4, 5$; and the plots in the third row show the number of subintervals in the adaptive discretization of $[-1, 1]$ as a function of m for $\lambda = 10^2, 10^3, 10^4, 10^5$. The plots in the column on the left concern experiments executed with the precision parameter ϵ taken to be 10^{-7}, while those on the right correspond to $\epsilon = 10^{-12}$.

So we expect the adaptive Levin method to divide $[-1, 1]$ into at least

$$\log(1/\delta) \sim \frac{\log(m\lambda)}{m-1} \tag{192}$$

subintervals. The algorithm will further divide the subintervals contained in $[-1, -\delta]$ and $[\delta, 1]$ until, on each of the resulting subintervals, the ratio of the maximum to minimum value of g' is small and h is well-represented via a Chebyshev expansion of small fixed order. The number of subintervals required for these conditions to be met depends only weakly on m and λ. The dependence on λ arises because the greater the distance δ between these subintervals and 0, the fewer subdivisions required, and the distance δ depends on λ.

When $\epsilon = 10^{-12}$, the cost of our algorithm is dominated by the need to represent $h(z)$. This depends only weakly on m and λ, and this behavior is reflected in the results shown in Figure 3. They indicate that the cost of the adaptive Levin method grows only very slowly with λ in this case, and that it is essentially independent of m.

When $\epsilon = 10^{-7}$, the difficulty of representing $h(x)$ is lower, and the running time of our algorithm is dominated by the number of subdivisions needed to ensure δ is sufficiently small, at least when m is small. This is on the order of $\log(m\lambda)/(m-1)$, and we see this behavior in the plot appearing on the left-hand side of the first row of Figure 3. As m increases, though, the cost of representing $h(z)$ begins to dominate the running time of the algorithm and it ceases to depend strongly on λ. This is reflected in the plot appearing on the lower-left corner of Figure 3.

The behavior of the adaptive Levin method in the presence of stationary points is somewhat complicated, but from this analysis and the experiments described above, it is safe to conclude that at worst the algorithm grows logarithmically with the frequency of g'.

7.4 Certain integrals involving the Bessel functions

In the experiments described in this subsection, we used the adaptive Levin method to evaluate the integrals

$$\begin{aligned}
I_{10}(\nu) &= \int_0^\infty \frac{J_\nu(x)}{\sqrt{x}}\,dx = \frac{\Gamma\left(\frac{\nu}{2}+\frac{1}{4}\right)}{\sqrt{2}\,\Gamma\left(\frac{\nu}{2}+\frac{3}{4}\right)}, \\
I_{11}(\lambda) &= \int_0^\infty Y_{\frac{1}{2}}(\lambda x)\ \exp(-x)\,dx = -\frac{\sqrt{\sqrt{\lambda^2+1}+1}}{\sqrt{\lambda^3+\lambda}}, \\
I_{12}(\lambda) &= \int_0^{\frac{\pi}{2}} J_{2\lambda}\left(2\lambda\cos(x)\right)\,dx = \frac{\pi}{2}J_\lambda^2(\lambda) \quad \text{and} \\
I_{13}(\lambda) &= \int_0^\infty J_0(\lambda x)J_{\frac{1}{2}}(\lambda x)\exp(-x)\sqrt{x}\,dx = \sqrt{\frac{-1+\sqrt{1+4\lambda^2}}{\pi\lambda+4\pi\lambda^3}}.
\end{aligned} \tag{193}$$

Each of the above formulas can be found either in [25] or [26].

In the first experiment, we sampled $l = 200$ equispaced points $x_1, x_2, \ldots, x_l$ in the interval $[1, 7]$. Then, for each $\nu = 10^{x_1}, \ldots, 10^{x_l}$, we constructed a phase function for the normal form

$$y''(x) + \left(1 + \frac{\frac{1}{4} - \nu^2}{x^2}\right) y(x) = 0 \tag{194}$$

of Bessel's differential equation using the algorithm of [17]. This gave us the following representations of the Bessel function of the first and second kinds of order ν:

$$J_\nu(x) = \sqrt{\frac{2}{\pi x}} \frac{\sin\left(\psi_\nu^{\text{bes}}(x)\right)}{\sqrt{\frac{d}{dx}\psi_\nu^{\text{bes}}(x)}} \quad \text{and} \quad Y_\nu(x) = \sqrt{\frac{2}{\pi x}} \frac{\cos\left(\psi_\nu^{\text{bes}}(x)\right)}{\sqrt{\frac{d}{dx}\psi_\nu^{\text{bes}}(x)}}. \tag{195}$$

The first of these representations was used, together with the adaptive Levin method, to evaluate $I_{10}(\nu)$. More explicitly, we took the input functions for the adaptive Levin method to be

$$g(x) = \psi_\nu^{\text{bes}}(x) \quad \text{and} \quad \text{and} \quad f(x) = \frac{1}{x}\sqrt{\frac{2}{\pi \frac{d}{dx}\psi_\nu^{\text{bes}}(x)}}. \tag{196}$$

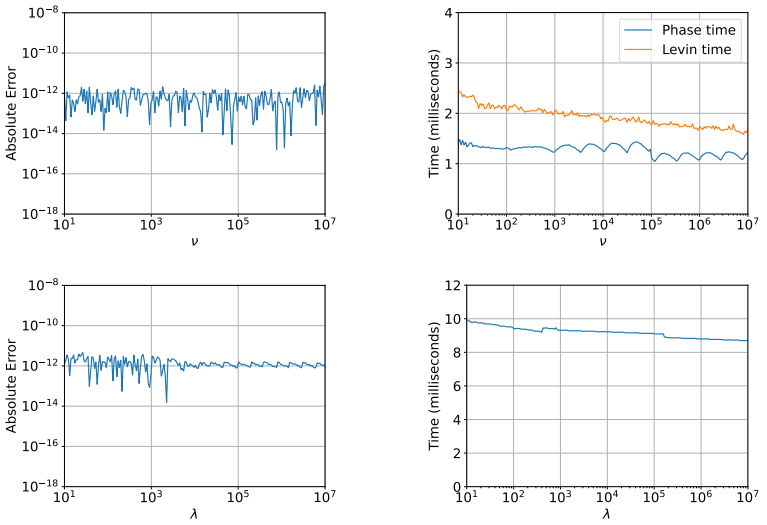

Fig. 4: The results of the first two experiments of Section 7.4. In the first row, the plot on the left gives the absolute error in the calculation of the integral $I_{10}(\nu)$ as a function ν and the plot on the right shows the time take by the adaptive Levin method and the time taken to construct the phase function as functions of ν. The plot at bottom left gives the absolute error in the obtained value of $I_{11}(\lambda)$ as a function of λ, and the bottom-right plot gives the time required to compute $I_{11}(\lambda)$, including the time required to construct any necessary phase functions, as a function of λ.

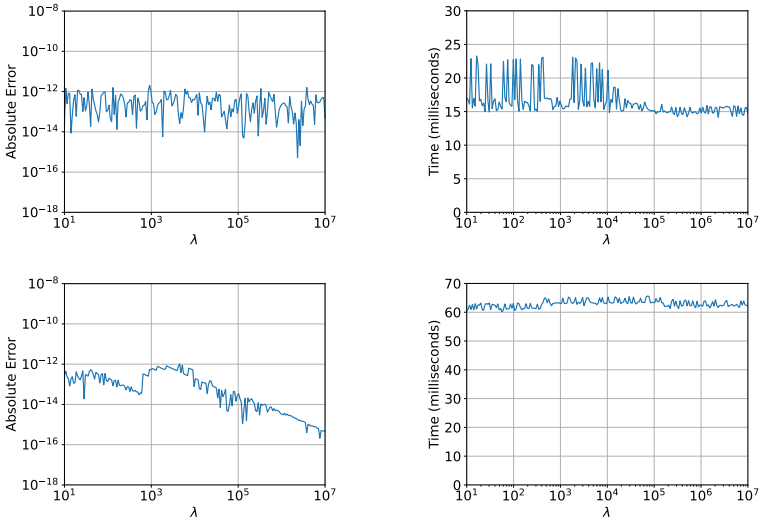

Fig. 5: The results of the last two experiments of Section 7.4. The first row pertains to $I_{12}(\lambda)$ while the second concerns $I_{13}(\lambda)$. In each row, the plot on the left gives the absolute error in the calculation of the integral as a function of λ and the plot on the right shows the total time required to compute the integral via the adaptive Levin method and to construct any necessary phase functions as a function of λ.

The results are given in the first row of Figure 4. Note that for this experiment, we report the time taken by the adaptive Levin method and the time required to construct the phase function separately.

We began our second experiment by sampling $l = 200$ equispaced points $x_1, \ldots, x_l$ in the interval $[1, 7]$. Then, for each $\lambda = 10^{x_1}, 10^{x_2}, \ldots, 10^{x_l}$, we constructed the phase function $\psi^{\text{bes}}_{1/2}$ and executed the adaptive Levin method with the input functions taken to be

$$g(x) = \psi^{\text{bes}}_{1/2}(\lambda x) \quad \text{and} \quad f(x) = \sqrt{\frac{2}{\pi}} \exp(-x) \sqrt{\frac{1}{\lambda x \, \frac{d}{dx} \psi^{\text{bes}}_{1/2}(\lambda x)}} \tag{197}$$

in order to evaluate $I_{11}(\lambda)$. The results are shown in the second row of Figure 4. The reported times include the cost of constructing the phase function as well as the time required by the adaptive Levin method.

We began our third experiment regarding Bessel functions by sampling $l = 200$ equispaced points $x_1, \ldots, x_l$ in the interval $[1, 7]$. Then, for each $\lambda = 10^{x_1}, 10^{x_2}, \ldots, 10^{x_l}$, we constructed a phase function $\psi^{\text{bes}}_{2\lambda}$ representing the Bessel functions of order 2λ and used the adaptive Levin method to evaluate

$I_{12}(\lambda)$; the input functions were taken to be

$$g(x) = \psi_{2\lambda}^{\text{bes}}(2\lambda\cos(x)) \quad \text{and} \quad f(x) = \sqrt{\frac{2}{\pi}}\sqrt{\frac{1}{2\lambda\cos(x)\,\frac{d}{dx}\psi_{2\lambda}^{\text{bes}}(2\lambda\cos(x))}}.$$

The results are shown in the first row of Figure 5. Once again, the reported times include the cost of constructing the necessary phase functions as well as the time required by the adaptive Levin method.

In our fourth experiment concerning Bessel functions, we first sampled $l = 200$ equispaced points $x_1, \ldots, x_l$ in the interval $[1, 7]$. Then, for each $\lambda = 10^{x_1}, 10^{x_2}, \ldots, 10^{x_l}$, we constructed the phase functions ψ_0^{bes} and $\psi_{1/2}^{\text{bes}}$, one representing the Bessel functions of order 0 and the other the Bessel functions of order $1/2$. Since

$$I_{13}(\lambda) = \frac{2}{\pi}\int_0^\infty \frac{\sin\left(\psi_0^{\text{bes}}(\lambda x)\right)}{\sqrt{\lambda x\,\frac{d}{dx}\psi_0^{\text{bes}}(\lambda x)}}\,\frac{\sin\left(\psi_{1/2}^{\text{bes}}(\lambda x)\right)}{\sqrt{\lambda x\,\frac{d}{dx}\psi_{1/2}^{\text{bes}}(\lambda x)}}\exp(-x)\sqrt{x}\,dx \tag{198}$$

and

$$\sin(x)\sin(y) = \frac{\cos(x-y) - \cos(x+y)}{2}, \tag{199}$$

we were able to compute I_{13} via the formula

$$I_{13}(\lambda) = \frac{2}{\lambda\pi}\,\frac{I_{13a}(\lambda) - I_{13b}(\lambda)}{2}, \tag{200}$$

where

$$I_{13a}(\lambda) = \int_0^\infty \frac{\cos\left(\psi_{1/2}^{\text{bes}}(x) - \psi_0^{\text{bes}}(x)\right)}{\sqrt{x\,\frac{d}{dx}\psi_0^{\text{bes}}(x)\,\frac{d}{dx}\psi_{1/2}^{\text{bes}}(x)}}\exp(-x)\,dx \tag{201}$$

and

$$I_{13b}(\lambda) = \int_0^\infty \frac{\cos\left(\psi_0^{\text{bes}}(x) + \psi_{1/2}^{\text{bes}}(x)\right)}{\sqrt{x\,\frac{d}{dx}\psi_0^{\text{bes}}(x)\,\frac{d}{dx}\psi_{1/2}^{\text{bes}}(x)}}\exp(-x)\,dx. \tag{202}$$

The integrals I_{13a} and I_{13b} were, of course, evaluated using the adaptive Levin method. The results are shown in the second row of Figure 5. The reported times include the cost of constructing the two necessary phase functions as well as the time required by the adaptive Levin method.

7.5 Comparison with adaptive Gaussian quadrature

In the experiment described in this subsection, we compared the performance of the adaptive Levin method to that of adaptive Gaussian quadrature by

evaluating the following integrals involving Bessel functions:

$$\begin{aligned} I_{14}(\lambda) &= \int_0^{10} J_0(\lambda x)\sqrt{\lambda x}\, dx, \\ I_{15}(\lambda) &= \int_0^{\pi} J_1(\lambda x^4)\log(x)\, dx \quad \text{and} \\ I_{16}(\lambda) &= \int_0^{100} J_1(\lambda x)\, Y_1(\lambda x)\, \lambda\, dx. \end{aligned} \tag{203}$$

We sampled $l = 200$ equispaced points $x_1, x_2, \ldots, x_l$ in the interval $[0, 6]$. Then, for each $\lambda = 10^{x_1}, \ldots, 10^{x_l}$, we used the adaptive Levin method combined with the algorithm of [17] to evaluate the integrals I_{14}, I_{15} and I_{16}. More explicitly, for each integral and each value of λ, we first used the method of [17] to construct a phase function representing the Bessel function or functions appearing in the integrals, and then applied the adaptive Levin method to the integral. The same integral was then evaluated using adaptive Gaussian quadrature. The results of this experiment are given in Figure 6. The first row of plots pertains to the integral I_{14}, the second row concerns I_{15} and the third concerns I_{16}. For each integral, we report the time required by each method and the absolute difference in the values obtained by each method. When reporting the time required by the adaptive Levin method, we include the cost to construct the phase function.

7.6 Certain integrals involving the associated Legendre functions

In the experiments described in this subsection, we used the adaptive Levin method to evaluate the integrals

$$\begin{aligned} I_{17}(\nu,\mu) &= \int_0^1 \widetilde{P}_\nu^\mu(x)(1-x^2)^{\frac{\mu}{2}}\, dx \\ &= \sqrt{\left(\nu+\frac{1}{2}\right)\frac{\Gamma(\nu+\mu+1)}{\Gamma(\nu-\mu+1)}}\,\frac{(-1)\mu 2^{-\mu-1}\sqrt{\pi}}{\Gamma\left(1+\frac{\mu}{2}-\frac{\nu}{2}\right)\Gamma\left(\frac{3}{2}+\frac{\mu}{2}+\frac{\nu}{2}\right)}, \\ I_{18}(\lambda) &= \int_0^1 \widetilde{P}_\lambda^{\frac{1}{2}}(x)\widetilde{Q}_\lambda^{\frac{1}{2}}(x)\, dx \quad \text{and} \\ I_{19}(\lambda) &= \int_0^{\frac{\pi}{2}} \widetilde{P}_\lambda^1(\cos(x))\, dx. \end{aligned}$$

Here, we use $\widetilde{P}_\nu^\mu$ and $\widetilde{Q}_\nu^\mu$ to denote normalized versions of the Ferrers functions of the first and second kinds of degree ν and order μ. For $\nu \geq \mu$, the usual Ferrers function P_ν^μ is the unique solution of the associated Legendre differential equation

$$(1-x^2)y''(x) - 2xy'(x) + \left(\nu(\nu+1) - \frac{\mu^2}{1-x^2}\right)y(x) = 0 \tag{204}$$

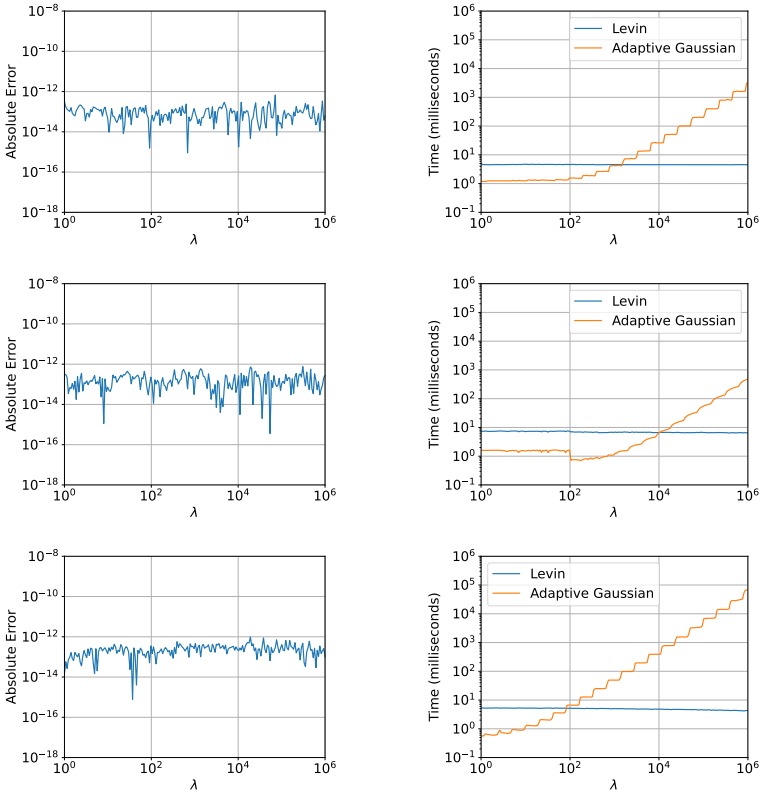

Fig. 6: The results of the experiment of Section 7.5. In the first row, the plot on the left gives the difference between the values of $I_{14}(\lambda)$ obtained using the adaptive Levin method and adaptive Gaussian quadrature as a function λ, while the plot on the right shows the time take by each method as a function of ν. The plots on the second and third rows give the same information, but pertain to $I_{15}(\lambda)$ and $I_{16}(\lambda)$, respectively.

which is regular at the singular point $x = 1$ and such that $P_\nu^\mu(1) = 1$. Because, for most values of the parameters ν and μ, P_ν^μ is exponentially decaying on some part of the interval $[0, 1]$, it can take on extremely large values. Accordingly, we prefer to work with the normalized Ferrers function

$$\widetilde{P}_\nu^\mu(x) = \sqrt{\left(\nu + \frac{1}{2}\right) \frac{\Gamma(\nu + \mu + 1)}{\Gamma(\nu - \mu + 1)}} P_\nu^\mu(x) \tag{205}$$

whose $L^2(-1, 1)$ norm is 1 when $n \geq m$ are integers. The Ferrers function Q_ν^μ of the second kind is (essentially) $\pi/2$ times the Hilbert transform of P_ν^μ and

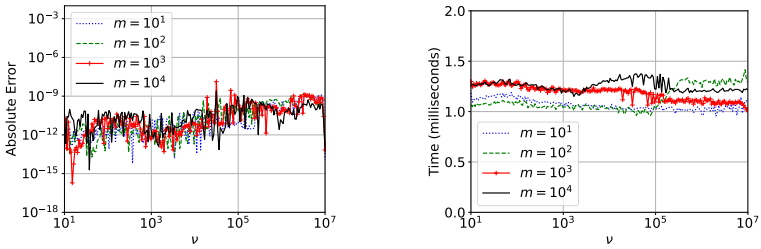

Fig. 7: The results of the first experiment of Section 7.6. The plots give the error in the calculated value of $I_{17}(m+\nu, m)$ and the time required to calculate it via the adaptive Levin method (including the time spent constructing the phase function) as functions of ν for $m = 10, 10^2, 10^3, 10^4$.

we define its normalized version via

$$\widetilde{Q}_\nu^\mu(x) = \frac{2}{\pi}\sqrt{\left(\nu+\frac{1}{2}\right)\frac{\Gamma(\nu+\mu+1)}{\Gamma(\nu-\mu+1)}}\,Q_\nu^\mu(x). \tag{206}$$

We refer the reader to Section 5.15 of [27] for a thorough discussion of the Ferrers functions.

Because (204) has singular points at ± 1, it is convenient to introduce the change of variables

$$z(w) = y(\tanh(w)), \tag{207}$$

which yields the new differential equation

$$z''(w) + \left(\nu(\nu+1)\operatorname{sech}^2(w) - \mu^2\right) z(w) = 0. \tag{208}$$

Applying the algorithm of [17] to (208) gives us the representations

$$\begin{aligned}\frac{\sin\left(\psi_{\nu,\mu}^{\mathrm{alf}}(w)\right)}{\sqrt{\frac{d}{dw}\psi_{\nu,\mu}^{\mathrm{alf}}(w)}} &= \sqrt{\frac{\pi}{2\nu+1}}\cos(\pi(\mu+1))\widetilde{P}_\nu^\mu\left(\tanh(w)\right)\\ &\quad -\sqrt{\frac{\pi}{2\nu+1}}\sin(\pi(\mu+1))\widetilde{Q}_\nu^\mu\left(\tanh(w)\right)\end{aligned} \tag{209}$$

and

$$\begin{aligned}\frac{\cos\left(\psi_{\nu,\mu}^{\mathrm{alf}}(w)\right)}{\sqrt{\frac{d}{dw}\psi_{\nu,\mu}^{\mathrm{alf}}(w)}} &= \sqrt{\frac{\pi}{2\nu+1}}\cos(\pi(\mu+1))\widetilde{P}_\nu^\mu\left(\tanh(w)\right)\\ &\quad +\sqrt{\frac{\pi}{2\nu+1}}\sin(\pi(\mu+1))\widetilde{Q}_\nu^\mu\left(\tanh(w)\right).\end{aligned} \tag{210}$$

In our first experiment, we sampled $l = 200$ equispaced points $x_1, \ldots, x_l$ in the interval $[1, 7]$. Then, for each $\nu = 10^{x_1}, \ldots, 10^{x_l}$ and each $m = 10, 10^2, 10^3, 10^4$, we constructed the phase function $\psi_{m+\nu,m}^{\mathrm{alf}}$ and applied the adaptive Levin

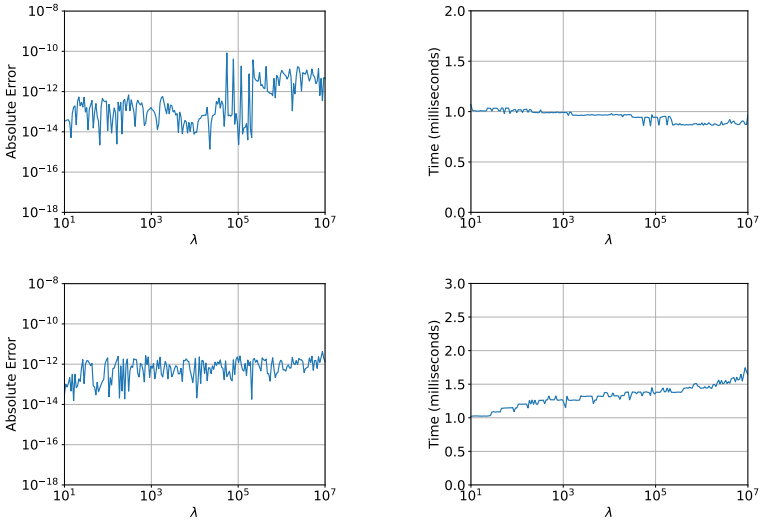

Fig. 8: The results of the last two experiments of Section 7.6. The first row pertains to $I_{18}(\lambda)$ while the second concerns $I_{19}(\lambda)$. In each row, the plot on the left gives the absolute error in the calculation of the integral as a function of λ and the plot on the right shows the total time required to compute the integral via the adaptive Levin method and to construct any necessary phase functions as a function of λ.

method to the integral

$$(-1)^{m+1}\sqrt{\frac{2\nu+2m+1}{\pi}}\int_0^\infty \frac{\sin\left(\psi^{\text{alf}}_{m+\nu,m}(w)\right)}{\sqrt{\frac{d}{dw}\psi^{\text{alf}}_{m+\nu,m}(w)}}\,\text{sech}(w)^{2+m}\,dw \tag{211}$$

in order to evaluate $I_{17}(m+\nu, m)$. We note that the associated Legendre functions are generally only defined when the degree is greater than or equal to the order, hence our decision to write the degree in the form $m+\nu$ with m the order of the associated Legendre function being integrated. Moreover, by choosing integer values of m we ensured that only the term involving the function of the first kind was nonzero in (209). The results are given in Figure 7. The timings reported there include both the cost to apply the adaptive Levin method and the time required to construct the phase function.

In our second experiment concerning the associated Legendre functions, we sampled $l = 200$ equispaced points $x_1, \ldots, x_l$ in the interval $[1, 7]$. Then, for each $\lambda = 10^{x_1}, \ldots, 10^{x_l}$, we constructed the phase function $\psi^{\text{alf}}_{\lambda,\frac{1}{2}}$ and applied the adaptive Levin method to the integral

$$\frac{2\lambda+1}{2\pi}\int_0^\infty \frac{\sin\left(2\psi^{\text{alf}}_{\lambda,\frac{1}{2}}(w)\right)}{\frac{d}{dw}\psi^{\text{alf}}_{\lambda,\frac{1}{2}}(w)}\,\text{sech}(w)^2\,dw, \tag{212}$$

which is equal to $I_{18}(\lambda)$ by virtue of the fact that $\sin(2x) = 2\sin(x)\cos(x)$. We took the input functions for the adaptive Levin method to be

$$g(x) = 2\psi^{\text{alf}}_{\lambda,\frac{1}{2}}(x) \tag{213}$$

and

$$f(x) = \frac{2\lambda+1}{2\pi}\frac{1}{\psi^{\text{alf}}_{\lambda,\frac{1}{2}}(\operatorname{arctanh}(\cos(x)))}. \tag{214}$$

The results are given in the first row of Figure 8. The timings reported there include both the cost to apply the adaptive Levin method and the time required to construct the required phase function.

In our third and final experiment regarding the associated Legendre functions, we sampled $l = 200$ equispaced points $x_1, \ldots, x_l$ in the interval $[1, 7]$. Then, for each $\lambda = 10^{x_1}, \ldots, 10^{x_l}$, we constructed the phase function $\psi^{\text{alf}}_{\lambda,1}$ via the algorithm of [17] and evaluated the integral $I_{19}(\lambda)$ via the adaptive Levin method. The input functions were taken to be

$$g(x) = \psi^{\text{alf}}_{\lambda,1}(\operatorname{arctanh}(\cos(x))) \tag{215}$$

and

$$f(x) = \sqrt{\frac{2\lambda+1}{2\pi}}\frac{1}{\sqrt{\psi^{\text{alf}}_{\lambda,1}(\operatorname{arctanh}(\cos(x)))}}. \tag{216}$$

The results are shown in the second row of Figure 8. The timings reported there include both the cost to apply the adaptive Levin method and the time required to construct the required phase function.

The runtime of evaluating the integral $I_{19}(\lambda)$ in this final experiment increases very mildly with λ, from around 1.0 ms for $\lambda = 10^1$ to around 1.7 ms for $\lambda = 10^7$. This is explained by the fact that the function $\tilde{P}^1_\lambda(\cos(x))$ appearing in the integrand of $I_{19}(\lambda)$ has a turning point, at which it resembles an error function of width $1/\lambda$. In order to resolve this feature, the adaptive Levin method must create on the order of $\log(1/\lambda)$ subintervals.

7.7 Certain integrals involving the Hermite polynomials

In the experiments of this subsection, we used the adaptive Levin method to evaluate the integrals

$$I_{20}(n) = \int_0^\infty \widetilde{H}_n(x)\exp\left(\frac{-x^2}{2}\right)dx,$$

$$I_{21}(n) = \int_0^\infty \widetilde{H}_n(x)(x)\cos(nx)\exp(-x)\,dx \quad \text{and}$$

$$I_{22}(n) = \int_0^\infty \widetilde{H}_n(\exp(x))\,dx,$$

where $\widetilde{H_n}$ denotes a normalized version of the Hermite polynomial of degree n. The Hermite polynomial H_n is the unique solution of

$$y''(x) - 2xy'(x) + 2ny(x) = 0 \tag{217}$$

which decays to 0 as $x \to \pm\infty$ and such that

$$H_n(0) = \frac{2^n\sqrt{\pi}}{\Gamma\left(\frac{1-n}{2}\right)}. \tag{218}$$

We define $\widetilde{H}_n$ via

$$\widetilde{H}_n(x) = \sqrt{\frac{\Gamma(n+1)}{2^n\sqrt{\pi}}}\exp\left(-\frac{x^2}{2}\right)H_n(x); \tag{219}$$

it is a solution of

$$y''(x) + \left(1 + 2n - x^2\right)y(x) = 0 \tag{220}$$

whose $L^2(-\infty,\infty)$ norm is 1. Applying the algorithm of [17] to (220) gives us the representation

$$\widetilde{H}_n(x) = C_n^{\text{herm}}\frac{\sin\left(\psi_n^{\text{herm}}(x)\right)}{\sqrt{\frac{d}{dx}\psi_n^{\text{herm}}(x)}} \tag{221}$$

of the normalized Hermite polynomial of degree n. The authors are not aware of a convenient formula for the constant C_n^{herm}; we determined it numerically after the phase function was constructed.

In our first experiment, we sampled $l = 200$ equispaced points $x_1, \ldots, x_l$ in the interval $[1, 7]$. Then, for each $n = \lfloor 10^{x_1}\rfloor, \ldots, \lfloor 10^{x_l}\rfloor$, we constructed the phase function ψ_n^{herm} and used it to evaluate $I_{20}(n)$. The results are given in the first row of Figure 9. The timings reported there include both the cost to apply the adaptive Levin method and the time required to construct the phase function.

In a second experiment concerning Hermite polynomials, we sampled $l = 200$ equispaced points $x_1, \ldots, x_l$ in the interval $[1, 7]$. Then, for each $n = \lfloor 10^{x_1}\rfloor, \ldots, \lfloor 10^{x_l}\rfloor$, we constructed the phase function ψ_n^{herm} and used it to evaluate the integrals

$$I_{21a}(n) = \int_0^\infty \frac{\sin\left(\psi_n^{\text{herm}}(x) - nx\right)}{\sqrt{\frac{d}{dx}\psi_n^{\text{herm}}(x)}}\exp(-x)\,dx \tag{222}$$

and

$$I_{21b}(n) = \int_0^\infty \frac{\sin\left(\psi_n^{\text{herm}}(x) + nx\right)}{\sqrt{\frac{d}{dx}\psi_n^{\text{herm}}(x)}}\exp(-x)\,dx \tag{223}$$

The value of $I_{21}(n)$ is then given by

$$I_{21}(n) = C_n^{\text{herm}}\frac{I_{21a}(n) + I_{21b}(n)}{2} \tag{224}$$

since

$$\sin(x)\cos(y) = \frac{\sin(x-y)+\sin(x+y)}{2}. \tag{225}$$

The results of this experiment are given in the second row of Figure 9. Again, the reported timings include both the cost to apply the adaptive Levin method and the time required to construct the phase function.

We began our third and final experiment regarding the Hermite polynomials by sampling $l = 200$ equispaced points $x_1, \ldots, x_l$ in the interval $[1, 7]$. Then, for each $n = \lfloor 10^{x_1} \rfloor, \ldots, \lfloor 10^{x_l} \rfloor$, we constructed the phase function ψ_n^{herm} and used it to evaluate $I_{22}(n)$. We took the input functions for the adaptive Levin method to be

$$g(x) = \psi_n^{\text{herm}}(\exp(x)) \quad \text{and} \quad f(x) = C_n^{\text{herm}} \frac{1}{\sqrt{\frac{d}{dx}\psi_n^{\text{herm}}(\exp(x))}}. \tag{226}$$

The results are shown in the third row of Figure 9. The timings reported there include both the cost to apply the adaptive Levin method and the time required to construct the phase function.

In the experiments of this subsection, the runtime can be seen to initially increase with λ, and then drop rapidly once λ exceeds some threshold. We have incorporated the cost of computing the phase function and evaluating the integral via the adaptive Levin method into the times which are reported, and this behavior is due to the cost of the constructing the phase functions. Indeed, this pattern is quite typical with phase function calculations. In the low-frequency regime, when λ is small, it can be the case that all phase functions for (217) oscillate, but they do so at low frequencies because λ is small. Once λ becomes sufficiently large, the existence of a nonoscillatory phase function which can be computed in time independent of λ is guaranteed by the analysis presented in [14]. Because of this, in the low-frequency regime, the running time of numerical algorithms based on phase functions tend to grow with frequency. However, once a certain frequency threshold is reached, the complexity of the phase functions becomes essentially independent of frequency, or even slowly decreasing with frequency.

7.8 Evaluation of Modal Green's functions

In this set of experiments, we used the adaptive Levin method to evaluate the azimuthal Fourier components of the Green's function

$$G(x, x') = \frac{\exp(ik|x-x'|)}{4\pi|x-x'|} \tag{227}$$

for the Helmholtz equation in three dimensions. These functions, which are known as the modal Green's functions for the Helmholtz equation, are given by

$$\frac{1}{2\pi}\int_{-\pi}^{\pi} \frac{\exp(ik|x-x'|)}{4\pi|x-x'|}\exp(-im\theta)\,d\theta. \tag{228}$$

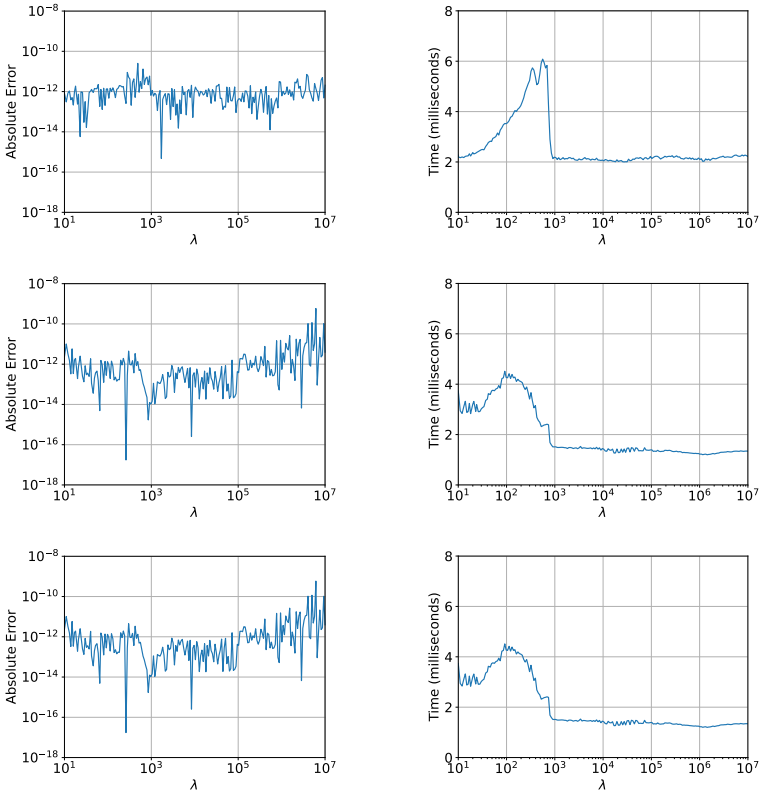

Fig. 9: The results of the experiments of Section 7.7. The first row pertains to $I_{20}(\lambda)$, the second concerns $I_{21}(\lambda)$ and the third pertains to $I_{22}(\lambda)$. In each row, the plot on the left gives the absolute error in the calculation of the integral as a function of λ and the plot on the right shows the total time required to compute the integral via the adaptive Levin method and to construct any necessary phase functions as a function of λ.

By introducing cylindrical coordinates $x = (r, \theta, z)$, $x' = (r', \theta', z')$ and letting $\phi = \theta - \theta'$, we can rewrite (228) as

$$I_{23}(\kappa, m, \alpha) = \frac{1}{4\pi^2} \int_{-\pi}^{\pi} \frac{\exp\left(-i\kappa\sqrt{1-\alpha\cos(\phi)}\right)}{\sqrt{1-\alpha\cos(\phi)}} \cos(m\phi)\, d\phi, \tag{229}$$

where

$$\kappa = kR_0, \quad \alpha = \frac{2rr'}{R_0}, \quad \text{and} \quad R_0^2 = r^2 + (r')^2 + (z-z')^2. \tag{230}$$

In the first experiment, we sampled $l = 200$ equispaced points $x_1, \ldots, x_l$ in the interval $[1, 7]$. Then, for each $m = 10^{x_1}, \ldots, 10^{x_l}$, $\kappa = 10^2, 10^3, 10^4, 10^5$ and

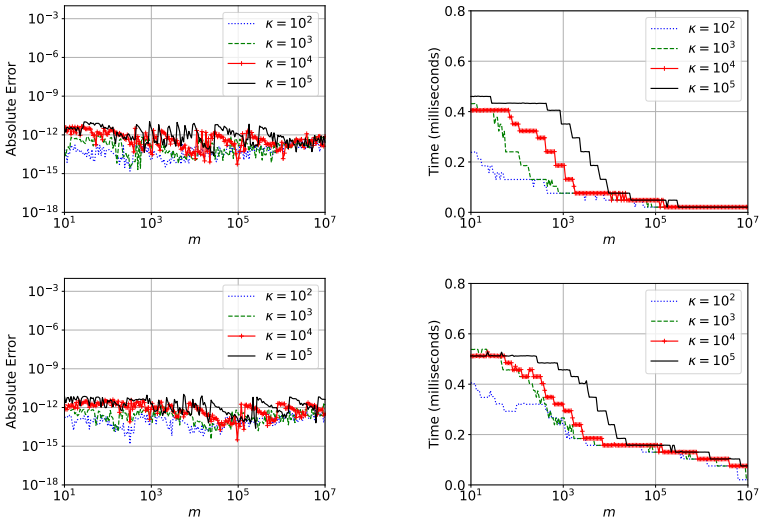

Fig. 10: The results of the first experiment of Section 7.8. The plot on the left-hand side of the first row gives the absolute error in the calculated value of $I_{23}(\kappa, m, \alpha)$ as a function of m for four values of κ in the case $\alpha = 0.5$. The plot on the right-hand side of the first row gives the time required to calculate $I_{23}(\kappa, m, \alpha)$ via the adaptive Levin method as a function of m for four values of κ in the case $\alpha = 0.5$. The plots in the second row give analogous data in the event $\alpha = 0.99$.

$\alpha = 0.5, 0.99$, we evaluated $I_{23}(\kappa, m, \alpha)$ using the adaptive Levin method and via adaptive Gaussian quadrature. Figure 10 gives the results.

In a second experiment, we sampled $l = 200$ equispaced points $x_1, \ldots, x_l$ in the interval $[1, 7]$. Then, for each $\kappa = 10^{x_1}, \ldots, 10^{x_l}$, $m = 10^2, 10^3, 10^4, 10^5$ and $\alpha = 0.5, 0.99$, we evaluated $I_{23}(\kappa, m, \alpha)$ using the adaptive Levin method and via adaptive Gaussian quadrature. In this experiment, the tolerance parameters for both the adaptive Levin method and our adaptive Gaussian quadrature code were set to $\epsilon_0\sqrt{\kappa}$, where ϵ_0 is machine zero for IEEE double precision arithmetic (about 2.22×10^{-16}). The value of $I_{23}(\kappa, m, \alpha)$ decreases, but not at a sufficient rate to completely compensate for the growth in its condition number, particularly when α is close to 1. Hence, the need to allow the tolerance parameter to increase with κ. Figure 11 gives the results.

A state-of-the-art method for evaluating the modal Green's functions is discussed in [28]. Amortizing over m, it is around 10 times more efficient than the adaptive Levin method in all cases. Notably, the performance of their algorithm does not change as α approaches 1, whereas the cost of the adaptive Levin method can increase significantly. Nonetheless, the adaptive Levin method is surprisingly competitive given that it is a general-purpose approach to evaluating oscillatory integrals and the algorithm of [28] is highly-specialized. Moreover, the adaptive Levin method can evaluate a single modal Green's

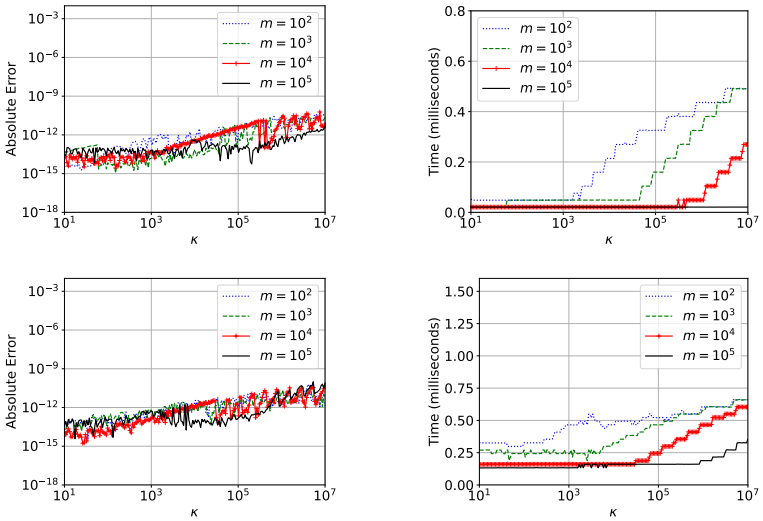

Fig. 11: The results of the second experiment of Section 7.8. The plot on the left-hand side of the first row gives the absolute error in the calculated value of $I_{23}(\kappa, m, \alpha)$ as a function of κ for four values of m in the case $\alpha = 0.5$. The plot on the right-hand side of the first row gives the time required to calculate $I_{23}(\kappa, m, \alpha)$ via the adaptive Levin method as a function of κ for four values of m in the case $\alpha = 0.5$. The plots in the second row give analogous data in the event $\alpha = 0.99$.

function in time independent of m and κ, while the algorithm of [28], when combined with certain recurrence relations, can only evaluate m modal Green's functions in $O(m)$ time, resulting in a constant amortized cost.

It is interesting to observe from the second column of Figure 11 that the runtime of the adaptive Levin method is initially constant with respect to κ up until $\kappa \approx m$, at which point the runtime begins to mildly increase with respect to κ. This is explained by the fact that the integrands of the modal Green's functions contain two oscillatory terms, one oscillating with frequency m and the other with frequency κ. When $\kappa < m$, there is little aliasing and few stationary points. Once $\kappa \geq m$, the aliasing between the two oscillatory terms begins to grow, and the number of stationary points quickly increases. The result is a mild growth in the cost of the adaptive Levin method, in agreement with the experiments of Subsection 7.9. An example showing some of these stationary points in the case $\kappa > m$ can be found in the phase-amplitude plot in Figure 13 of [28].

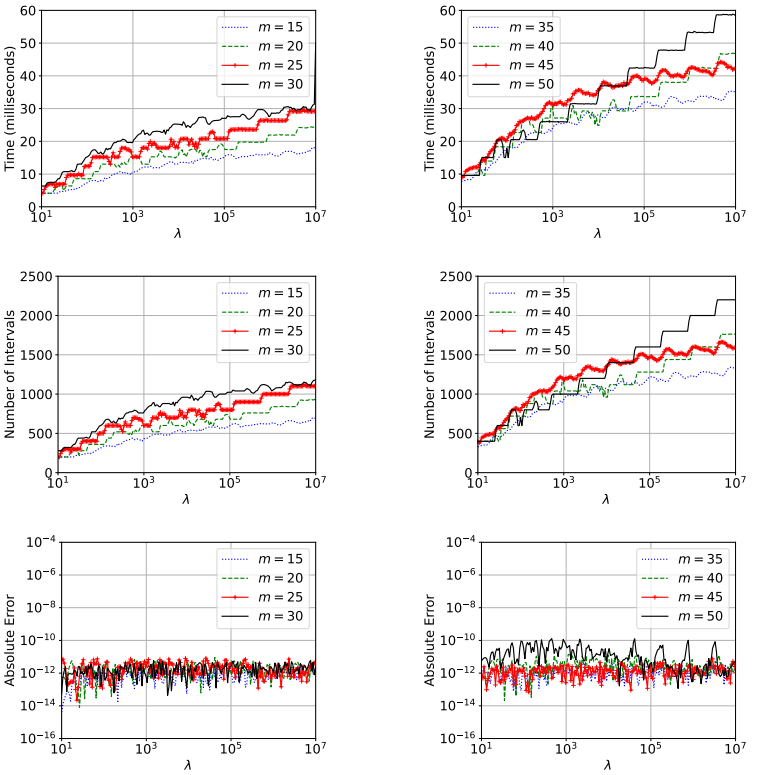

Fig. 12: The results of the experiment of Section 7.9. The plots in the first row give the time taken by the adaptive Levin method as a function of λ for the various values of m considered. Those in the second row give the number of intervals in the adaptively determined subdivision of $[-1, 1]$ used to compute the integral I_{24} as a function of λ for the values of m considered. The third row of plots give the error in the calculated value of $I_{24}(\lambda, m)$ as a function of λ for $m = 15, 20, 25, 30, 35, 40, 45, 50$.

7.9 An integral with many stationary points

In this final experiment, we considered the integral

$$I_{24}(\lambda, m) = \int_{-1}^{1} \exp\left(i\lambda \cos^2\left(\frac{\pi}{2} mx\right)\right) \frac{1}{1+x^2}\, dx, \tag{231}$$

which has m stationary points. We sampled $l = 200$ equispaced points $x_1, \ldots, x_l$ in the interval $[1, 7]$ and, for each $\lambda = 10^{x_1}, 10^{x_2}, \ldots, 10^{x_l}$ and $m = 15, 20, 25, 30, 35, 40, 45, 50$, we evaluated $I_{24}(\lambda, m)$ using the adaptive Levin method.

Figure 12 presents the results. We see that, when applied to I_{24}, the running time of the adaptive Levin method grows sublogarithmically with λ for all of the values of m considered. The cost also increases quite mildly as a function

of the number of stationary points. It is notable that the method is able to evaluate $I_{24}\left(10^7, 20\right) \approx 4.72 \cdot 10^{-4}$ — a highly oscillatory integral with 50 stationary points — to 11 digit absolute precision accuracy and 7 digit relative precision accuracy, in approximately 50 milliseconds.

8 Conclusions

We have shown that the Levin method does not suffer from numerical breakdown when the magnitude of g' is small or when g' has zeros, which explains the effectiveness of adaptive Levin methods. We have also presented numerical experiments indicating that the adaptive Levin method of this paper can accurately and rapidly evaluate a large class of oscillatory integrals, including many with singularities and stationary points. We have further demonstrated that combining the adaptive Levin method with the algorithm of [16, 15] allows for the efficient evaluation of many integrals involving oscillatory solutions of differential equations. This class includes integrals involving most of the classical special functions, as well as combinations of such functions and compositions of such functions with slowly-varying functions.

As the experiments of Section 7.8 indicate, specialized techniques designed for particular narrow classes of oscillatory integrals are often faster than the adaptive Levin scheme of this paper. However, the numerical experiments described in Section 7 show that the adaptive Levin method provides an efficient general-purpose mechanism for evaluating a huge class of oscillatory integrals. It appears to have roughly the same behavior when applied to oscillatory integrals as adaptive Gaussian quadrature does when used to evaluate integrals with smoothly varying integrands.

We note that there are obvious implications of the adaptive Levin method for the rapid application of special function transforms and the solution of second order linear inhomogeneous differential equations that should be thoroughly investigated.

9 Acknowledgements

KS was supported in part by the NSERC Discovery Grants RGPIN-2020-06022 and DGECR-2020-00356. JB was supported in part by NSERC Discovery grant RGPIN-2021-02613.

References

[1] Levin, D.: Procedures for computing one- and two-dimensional integrals of functions with rapid irregular oscillations. Mathematics of Computation **38**, 531–538 (1982)

[2] Li, J., Wang, X., Wang, T.: A universal solution to one-dimensional oscillatory integrals. Science in China Series F: Information Sciences **51**, 1614–1622 (2008)

[3] Li, J., Wang, X., Wang, T., Xiao, S.: An improved Levin quadrature method for highly oscillatory integrals. Applied Numerical Mathematics **60**(8), 833–842 (2010)

[4] Levin, D.: Analysis of a collocation method for integrating rapidly oscillatory functions. Journal of Computational and Applied Mathematics **78**(1), 131–138 (1997)

[5] Ashton, A.: Cauchy data for levin's method. IMA Journal of Numerical Analysis, 106 (2024)

[6] Moylan, A.J.: Highly oscillatory integration, numerical wave optics, and the gravitational lensing of gravitational waves. PhD thesis, The Australian National University (2008)

[7] Hascelik, A.I., Boy, O., Gercek, A.S.: An efficient adaptive levin-type method for highly oscillatory integrals. Applied Mathematical Sciences **8**(138), 6889–6908 (2014)

[8] Levin, D.: Fast integration of rapidly oscillatory functions. Journal of Computational and Applied Mathematics **67**, 95–101 (1996)

[9] Miller, P.D.: Applied Asymptotic Analysis. American Mathematical Society, Providence, Rhode Island (2006)

[10] Wasow, W.: Asymptotic Expansions for Ordinary Differential Equations. Dover, New York (1965)

[11] Spigler, R., Vianello, M.: The phase function method to solve second-order asymptotically polynomial differential equations. Numerische Mathematik **121**, 565–586 (2012)

[12] Spigler, R.: Asymptotic-numerical approximations for highly oscillatory second-order differential equations by the phase function method. Journal of Mathematical Analysis and Applications **463**, 318–344 (2018)

[13] Spigler, R., Vianello, M.: A numerical method for evaluating the zeros of solutions of second-order linear differential equations. Mathematics of Computation **55**, 591–612 (1990)

[14] Bremer, J., Rokhlin, V.: Improved estimates for nonoscillatory phase functions. Discrete and Continuous Dynamical Systems, Series A **36**, 4101–4131 (2016)

[15] Aubry, M., Bremer, J.: A solver for linear scalar ordinary differential equations whose running time is bounded independent of frequency. arXiv:2311.08578 (2023)

[16] Bremer, J.: On the numerical solution of second order differential equations in the high-frequency regime. Applied and Computational Harmonic Analysis **44**, 312–349 (2018)

[17] Bremer, J.: Phase function methods for second order linear ordinary differential equations with turning points. Applied and Computational Harmonic Analysis **65**, 137–169 (2023)

[18] Mason, J.C., Hanscomb, D.C.: Chebyshev Polynomials. Chapman and Hall, New York, New York (2003)

[19] Boyd, J.P.: Approximation of an analytic function on a finite real interval by a bandlimited function and conjectures on properties of prolate spheroidal functions. Applied and Computational Harmonic Analysis **15**(2), 168–176 (2003)

[20] Davis, P.: Interpolation and Approximation. Dover, New York, New York (1975)

[21] NIST Digital Library of Mathematical Functions, (2024). F. W. J. Olver, A. B. Olde Daalhuis, D. W. Lozier, B. I. Schneider, R. F. Boisvert, C. W. Clark, B. R. Miller, B. V. Saunders, H. S. Cohl, and M. A. McClain, eds.

[22] Bateman, H., Erdélyi, A.: Higher Transcendental Functions vol. II. McGraw-Hill, New York, New York (1953)

[23] Zhao, M., Serkh, K.: On the approximation of singular functions by series of non-integer powers. arXiv:2308.10439 (2023)

[24] Olver, F.W.J.: A new method for the evaluation of zeros of Bessel functions and of other solutions of second-order differential equations. Proc. Cambridge Philos. Soc., 570–580 (1950)

[25] Gradshteyn, I.S., Ryzhik, I.M.: Table of Integrals, Sums, Series and Products, 7th edn. Academic Press, Amsterdam (2007)

[26] Bateman, H., Erdélyi, A.: Tables of Integrals vol. II. McGraw-Hill, New York, New York (1954)

[27] Olver, F.W.J.: Asymptotics and Special Functions. A.K. Peters, Wellesley, Massachusetts (1997)

[28] Garritano, J., Kluger, Y., Rokhlin, V., Serkh, K.: On the efficient evaluation of the azimuthal Fourier components of the Green's function for Helmholtz's equation in cylindrical coordinates. Journal of Computational Physics **471**, 111585 (2022)